THE UNIVERSITY OF MIAMI

The Baroclinic Structure of the Florida Current

BY

William O. Stubbs, Jr.

A THESIS

Submitted to the Faculty
of the University of Miami
in partial fulfillment of the requirements for
the degree of Master of Science

Coral Gables, Florida

June 1971

THE UNIVERSITY OF MIAMI

The Baroclinic Structure of the Florida Current

BY

William O. Stubbs, Jr.
LCDR, U.S. Navy

A THESIS

Submitted to the Faculty
of the University of Miami
in partial fulfillment of the requirements for
the degree of Master of Science

Coral Gables, Florida

June 1971

STUBBS, WILLIAM OLAN, JR. (M.S., Physical Oceanography)

The Baroclinic Structure of the Florida Current. (June 1971). Abstract of a Master's Thesis at the University of Miami. Thesis supervised by Professor Christopher N.K. Mooers.

Nine consecutive days of free-fall, STD data are analyzed in a study of the baroclinic structure of the Florida Current. Mean values averaged over the nine days are used to reduce tidal aliasing.

A southward flow is confirmed during the nine day period. Based on this data and previous works, the southward flow appears to be of a transient nature.

Comparison of the directly measured and geostrophically computed current and transport indicates that the Florida Current is essentially in geostrophic balance.

ACKNOWLEDGEMENTS

My sincerest thanks go to Dr. William S. Richardson, NOVA University, who not only made the data available, but also provided many helpful suggestions during the preparation of this thesis. I am deeply grateful to the members of my thesis committee: Dr. Walter Düing, who suggested the topic, Dr. Claes Rooth and Dr. Harry A. DeFerrari. In particular, I express my sincere appreciation and gratitude to Dr. Christopher N.K. Mooers, my thesis committee chairman. Without his wise guidance, timely suggestions and constant encouragement, this work might never have been completed. A special thanks to Manuel Bascuas for his help in computer programming. And to Joyce Stubbs, the ultimate in gratitude is due.

The financial support for this study was provided by the Office of Naval Research Contract No. N00014-67-A-0201-0013, Project No. NR 083-060.

William O. Stubbs, Jr.

Coral Gables, Florida
June 1971

TABLE OF CONTENTS

	Page
LIST OF TABLES	v
LIST OF FIGURES	vi
LIST OF APPENDICES	viii
I. INTRODUCTION	1
II. METHODS	3
A. Data Acquisition	3
B. Data Analysis	4
C. Analysis of Errors	24
III. RESULTS	28
A. Comparison of Direct Measurements and Geostrophic Calculations	28
B. Features of the Florida Current	36
IV. SUMMARY AND CONCLUSIONS	47
A. Summary	47
B. Conclusions	48
LITERATURE CITED	51
APPENDIX	54

LIST OF TABLES

TABLE		Page
I.	Free-fall Instrument Data	6
II.	Time of Observation and Depth of Probe for Free-Fall Transects	7

LIST OF FIGURES

FIGURE Page

1. Station locations 5
2. Mean temperature (C°) section 8
3. Mean salinity (‰) section 9
4. Mean sigma-t section 10
5. Observed velocity profile for stations 5 and 7 12
6. Mean observed axial velocity (cm/sec) 14
7. Mean dynamic depth difference (ΔD) 17
8. Depth of no motion 19
9. Mean axial velocity (cm/sec), observed and geostrophic (depth of no motion by Defant's method) 20
10. Mean axial velocity (cm/sec), observed and geostrophic ($V_{geostrophic} = V_{observed}$ at surface) 21
11. Mean axial velocity (cm/sec), observed and geostrophic ($V_{geostrophic} = 0$ at bottom) 22
12. Mean axial velocity (cm/sec), observed and geostrophic (depth of no motion = 400 meters) 23
13. Standard deviation for temperature (C°), salinity (‰), and sigma-t (σ_t units) 27
14. Mean surface velocity (cm/sec), observed and geostrophic (hybrid depth of no motion) 29
15. Mean axial velocity (cm/sec), observed and geostrophic (hybrid depth of no motion) 31
16a. Velocity profile (cm/sec), observed and geostrophic (hybrid depth of no motion), stations 2, 3 and 4 32

FIGURE Page

16b. Velocity profile (cm/sec), observed and geostrophic (hybrid depth of no motion), stations 5 and 7 33

16c. Velocity profile (cm/sec), observed and geostrophic (hybrid depth of no motion), stations 8, 10 and 11 34

17. Transport per unit width (m^2/sec), observed and geostrophic (hybrid depth of no motion), stations 3, 7 and 10. Dots indicate free-fall data 35

18. Thermal wind ratio section 37

19. Baroclinic stability parameter section 39

20. Richardson number section 40

21. T-S curve, stations 2, 6 and 10 41

22. Mean observed downstream transport (m^3/sec) and surface velocity (cm/sec) with standard errors 43

23. Mean observed cross-stream transport (m^3/sec) with standard errors 46

LIST OF APPENDICES

APPENDIX Page

A. Tidal aliasing computations 54

I. INTRODUCTION

There have been several previous attempts to determine the validity of the geostrophic approximation in the Florida Current. This thesis is a further examination of the baroclinic structure of the Florida Current using free-fall, STD instrument data. For a period of nine consecutive days in May-June 1969 direct measurements of the transport versus depth of the Florida Current between Miami and Bimini were made by Dr. William S. Richardson (NOVA University) using free-fall instruments. At the majority of the stations occupied, one probe was equipped with the self-contained STD instrument.

A comparison is made of the average velocity structure determined by differentiating the mean transport versus depth curves and of the structure determined by geostrophic calculations based on the mean density field. To first order, geostrophic equilibrium, i.e. a balance between the Coriolis and pressure gradient forces, holds for most large-scale oceanic flows.

The first comparison of the observed and computed velocity fields in the Florida Current was made by Wust (1924) in which he used the direct measurements of Pillsbury (1890). Considering that the geostrophic calculations were based on a density field determined from three independent sources, the agreement between the measured and computed velocity fields was surprisingly good. The direct measurements of the current field by free-fall instruments (Richardson and Schmitz, 1965)

have led to more recent comparisons. Broida (1966) used a quasi-synoptic density field determined from hydrographic stations, and his computations showed a biaxial structure in the Florida Current while the direct measurements indicated a single axis. The discrepancy was attributed to aliasing of the hydrographic data by internal tides. A time averaged comparison of data taken during the summer months of 1965 and 1966 was made by O'Brien (1967). Using a mean T-S correlation, the density field was determined from the observed temperature only. O'Brien's analysis confirmed the validity of the geostrophic approximation in the Florida Current.

The free-fall, STD instrument provides for the first time the simultaneous measurement of the transport of all three of the density parameters: salinity, temperature, and pressure. By time averaging this synoptic data, tidal effects are further reduced. Thus, a rare opportunity exists to compare accurately the directly measured and the geostrophically computed velocity fields.

With an input of geographical station locations, water depths, and the values of observed velocity and density versus depth, the output of the CHARSECT computer program (Mooers, 1970) includes the following baroclinic parameters:

(1) the thermal wind ratio, which described the degree to which a flow is geostrophic,

(2) the baroclinic stability parameter, which tests the criticality of the isopycnal slopes, and

(3) the Richardson number, which describes the dynamic stability of the flow.

II. METHODS

A. DATA ACQUISITION

The free-fall technique yields volume transport per unit width versus depth and surface velocity data. When the free-fall instrument is equipped with the STD package, a continuous trace of salinity and temperature versus depth is also available. The free-fall technique employs weighted instruments that fall (attaining their terminal velocity of 2 m/sec within a few meters after release) to a pre-selected depth where the ballast weights are released, and the instrument returns to the surface under its own buoyancy (attaining their terminal velocity again within a few meters of ballast release). The precise recording of time and position of release and recovery provide the information necessary for measuring the depth-dependent transport and the surface velocity. At each station one drop is made to the bottom, and one to three drops are made to pre-selected depths. Since it is necessary to determine the horizontal deflection of the free-fall instrument, the navigational system is the controlling factor. The system used is Hifix (Decca Navigational System), where the master station is located on the vessel and the two slave stations on the western side of the Florida Straits. The range of the system is approximately 250 km with a precision of ± 1 meter on the western side of the Straits and ± 2 meters on the eastern side. A small, high speed vessel is used in conducting the measurements.

The data for this thesis were obtained from observations made over a nine-day period from 27 May 1969 through 4 June 1969 by Dr. W. S.

Richardson (NOVA University). A series of thirteen stations were occupied on a section from Miami to Bimini (Figure 1). Despite the short crossing time (7 to 8 hours) for a transect as compared to a typical hydrographic transect (20 to 24 hours), the distorting influence of tidal motions remains an important factor. In an effort to reduce this tidal aliasing, the station times were varied as practicable by starting transects at Miami and Bimini on alternate days. Tables I and II describe the free-fall instrument data that were used. Those observations that included an STD drop are indicated in Table II.

B. DATA ANALYSIS

The first step in determining the density field was the digitizing at ten meter intervals of salinity and temperature values from each free-fall STD trace. At each station the mean values of salinity and temperature at these intervals were computed for the nine day period. These mean values were used as the input to the standard hydrographic computer program.[1] The output of this program included sigma-t, specific volume anomaly, and dynamic depth. The cross stream sections of mean temperature, salinity, and σ_t (Figures 2, 3 and 4) are plotted with the observed current axis superimposed.

Mean values of observed transport versus depth, rather than daily values, were used to compute observed velocity.[2] With the volume

---

[1]Mean value is defined as the nine day average.

[2]An observed quantity is either a directly measured quantity (such as surface velocity) or a quantity (such as sub-surface velocity) directly computed from the free-fall measurement of volume transport.

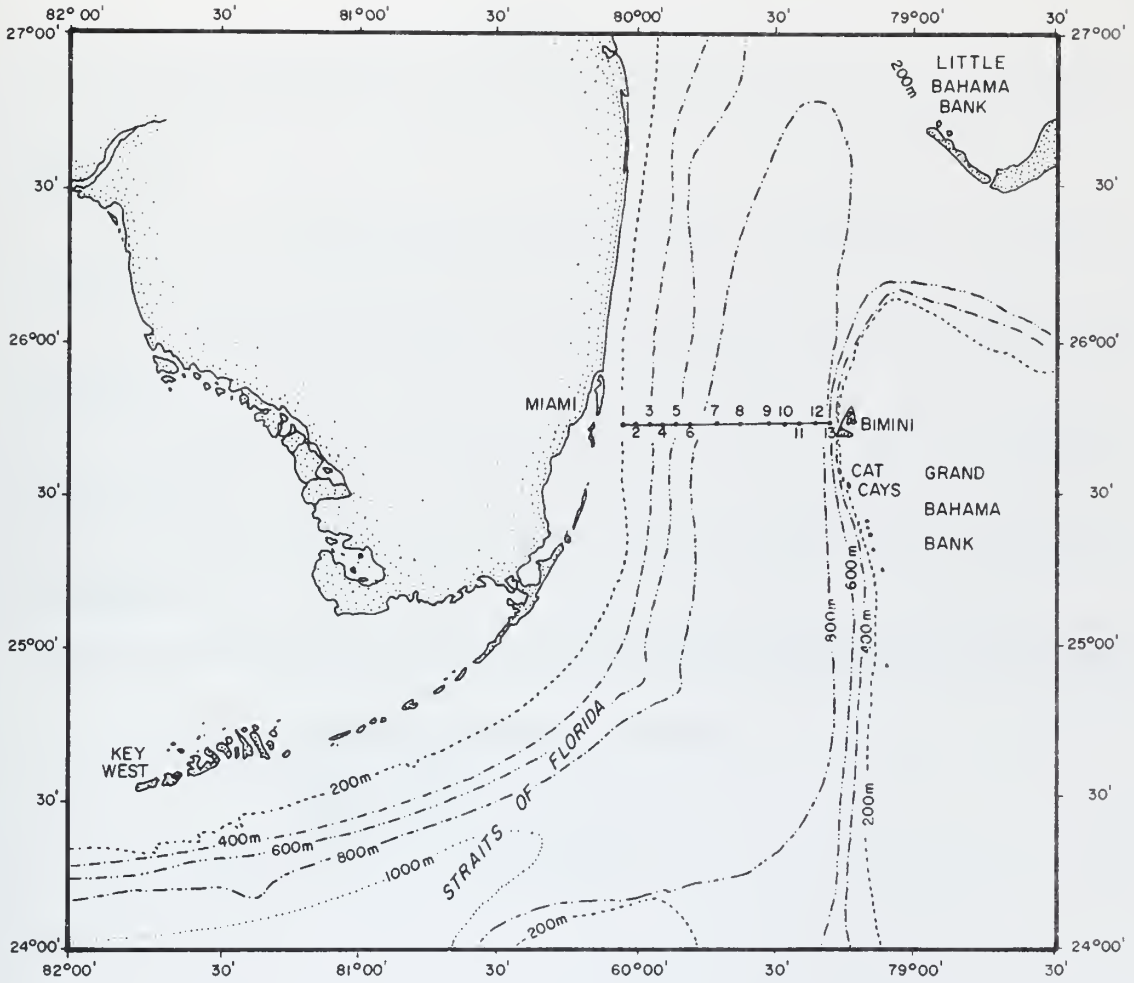

Figure 1. Station locations.

TABLE I

Station Number	1	2	3	4	5	6	7	8	9	10	11	12	13
Distance from reference point (km)	10	15	20	25	30	35	45	55	65	70	75	80	83
Maximum depth (m)	135	285	345	350	340	665	765	795	830	790	735	580	395
Average number of drops per station occupation	1	3	4	4	4	4	4	4	4	4	4	3	3
Total number of station occupations	8	9	9	8	9	9	9	9	8	8	9	6	5
Total number of observations with STD	5	6	6	6	7	7	7	6	5	5	4	3	4

Free-fall Instrument Data: Miami-Bimini

Dates: 27 May 1969 through 4 June 1969

Reference Point: Lat. 25°44.5'N

Long. 80°08.8'W

TABLE II

STATION NUMBER		1	2	3	4	5	6	7	8	9	10	11	12	13
DATE OF TRANSECT														
	Time of occupation	STD 0745	STD 0812	STD 0900	STD 0930	STD 1020	STD 1115	STD 1215	STD 1255		STD 1440	STD 1530		
27 May	Depth of probes	122	84	103	104	102	173	173	171		340	170		
			176	163	175	224	361	360	387		608	332		
			283	288	323	269	448	588	795		780	532		
				325	345	330	645	755						
	Time of occupation		STD 1428	STD 1355		STD 1320	STD 1240	STD 1120	STD 1045	STD 0940	STD 0905	STD 0810	STD 0750	STD 0655
28 May	Depth of probes		97	86		135	239	180	177	169	110	176	84	86
			154	94		166	349	341	346	338	357	354	320	181
			270	329		335	437	423	563	414	644	512	578	395
							650	758	785	818	782	721		
	Time of occupation	STD 0806	STD 0850	STD 0900	STD 0942	STD 1018	STD 1048	STD 1150	STD 1245	STD 1340	STD 1442	STD 1512	STD 1600	STD 1630
29 May	Depth of probes	120	88	82	88	91	173	176	173	172	165	191	99	94
			183	167	173	164	393	364	373	329	385	380	315	172
			280	337	344	328	463	605	539	515	563	705	570	388
				340		335	657	747	773		780			
	Time of occupation	STD 1348	STD 1324	STD 1248	STD 1218	STD 1148	STD 1112	STD 1018	STD 0918	STD 0830	STD 0748	STD 0712	STD 0636	STD 0612
30 May	Depth of probes	118	88	92	95	95	181	177	231	233	177	170	96	98
			183	171	225	175	372	351	357	344	354	385	327	177
			270	265	330	326	494	598	520	525	523	695	570	
				320	350	340	636	748	780	806	776			
	Time of occupation	0710	0730	0810	0930	1000	1030	1115	1200	1300	1330	1350	1415	1430
31 May	Depth of probes	133	95	99	93	102	91	96	95	93	92	90	90	91
			179	235	185	134	172	166	160	160	208	167	372	133
			277	277	316	310	607	600	613	673	610	474	573	395
				326	350	336	662	754	782	814	765	733		
	Time of occupation	1150	1130	1120		1040	1020	0945	0900	0830	0730	0710	0630	
1 June	Depth of probes	94	278	97		90	94	98	95	103	95	86	93	
				160		158	177	170	173	152	176	721	290	
				331		337	650	763	783	812	777			
	Time of occupation	STD 1730	STD 0800	STD 0850	STD 0920	STD 1000	STD 1045	STD 1140	STD 1345	STD 1520	STD 1730	STD 1805		
2 June	Depth of probes	125	87	89	84	89	91	89	115	86	87	158		
			169	176	176	228	165	165	242	172	171	310		
			275	250	328	278	443	480	483	509	465	679		
				340	340	340	658	548	780	800	737			
								750						
	Time of occupation				STD 1555	STD 1530	STD 1450	STD 1400	STD 1312	STD 1215	STD 0840	STD 0700	STD 0615	STD 0530
3 June	Depth of probes	128	92	89	99	84	93	145	96	93	96	81	240	34
			181	182	171	178	243	167	161	187	144	169	288	183
			282	255	282	291	428	510	488	236	182	367	580	395
					340	330	645	750	788	466	470	610		
										810	780			
	Time of occupation	STD 0842	STD 0906	STD 0930	STD 1012	STD 1042	STD 1118	STD 1236	STD 1324	STD 1430				
4 June	epth of probes	123	96	96	92	85	154	166	230	228				
			170	172	187	175	390	378	401	363				
			268	265	303	330	644	755	780	803				
				342	342									

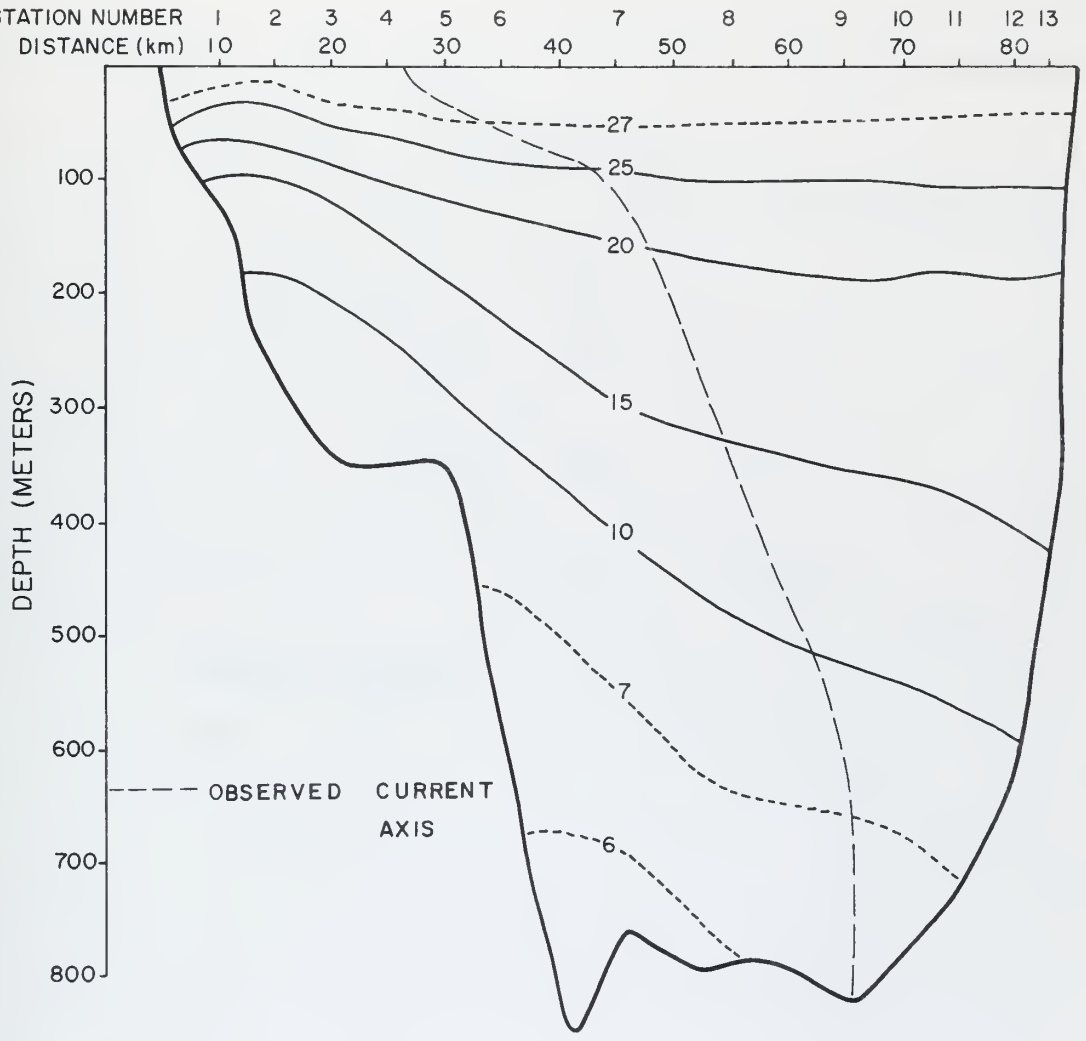

Figure 2. Mean temperature (C^{o}) section.

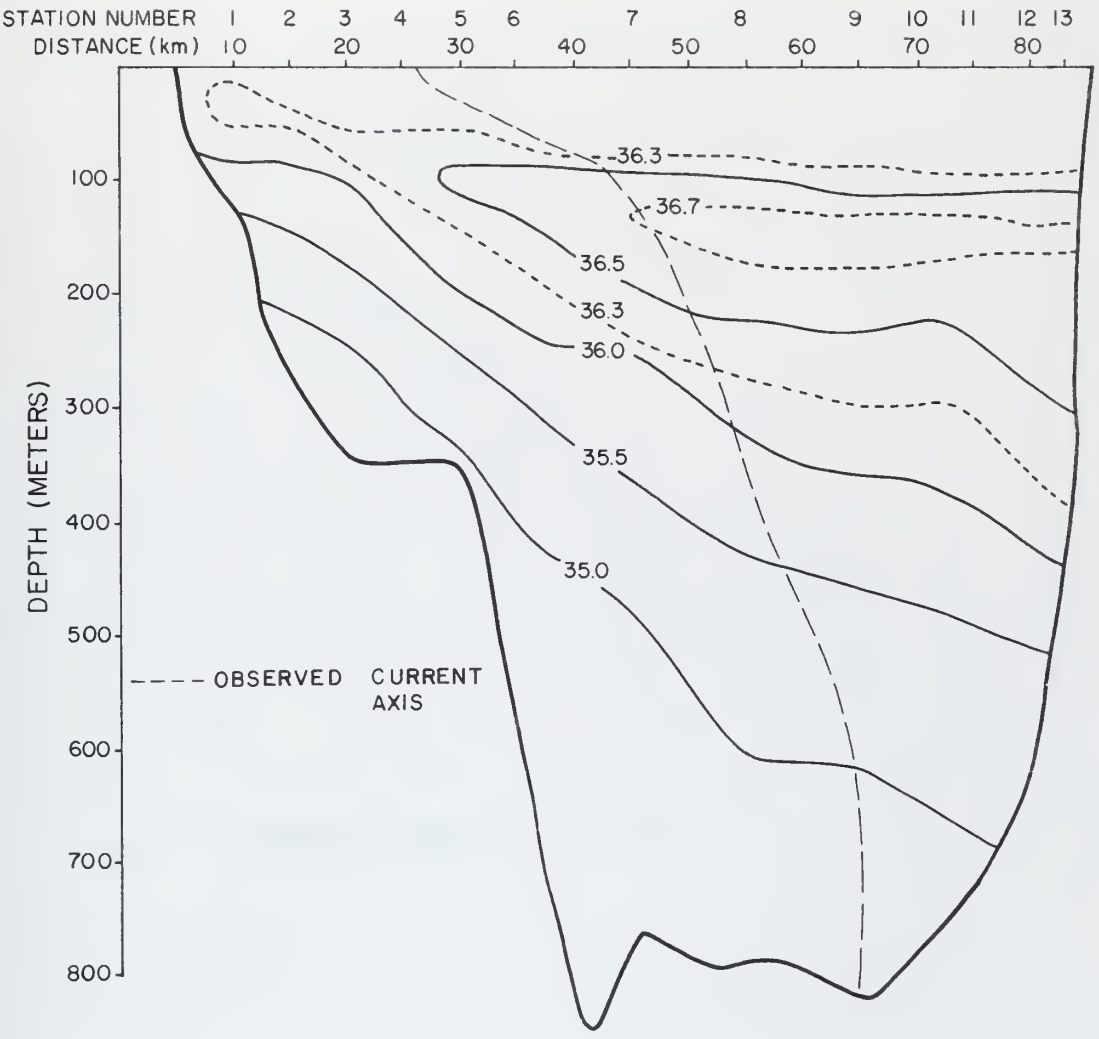

Figure 3. Mean salinity (‰) section.

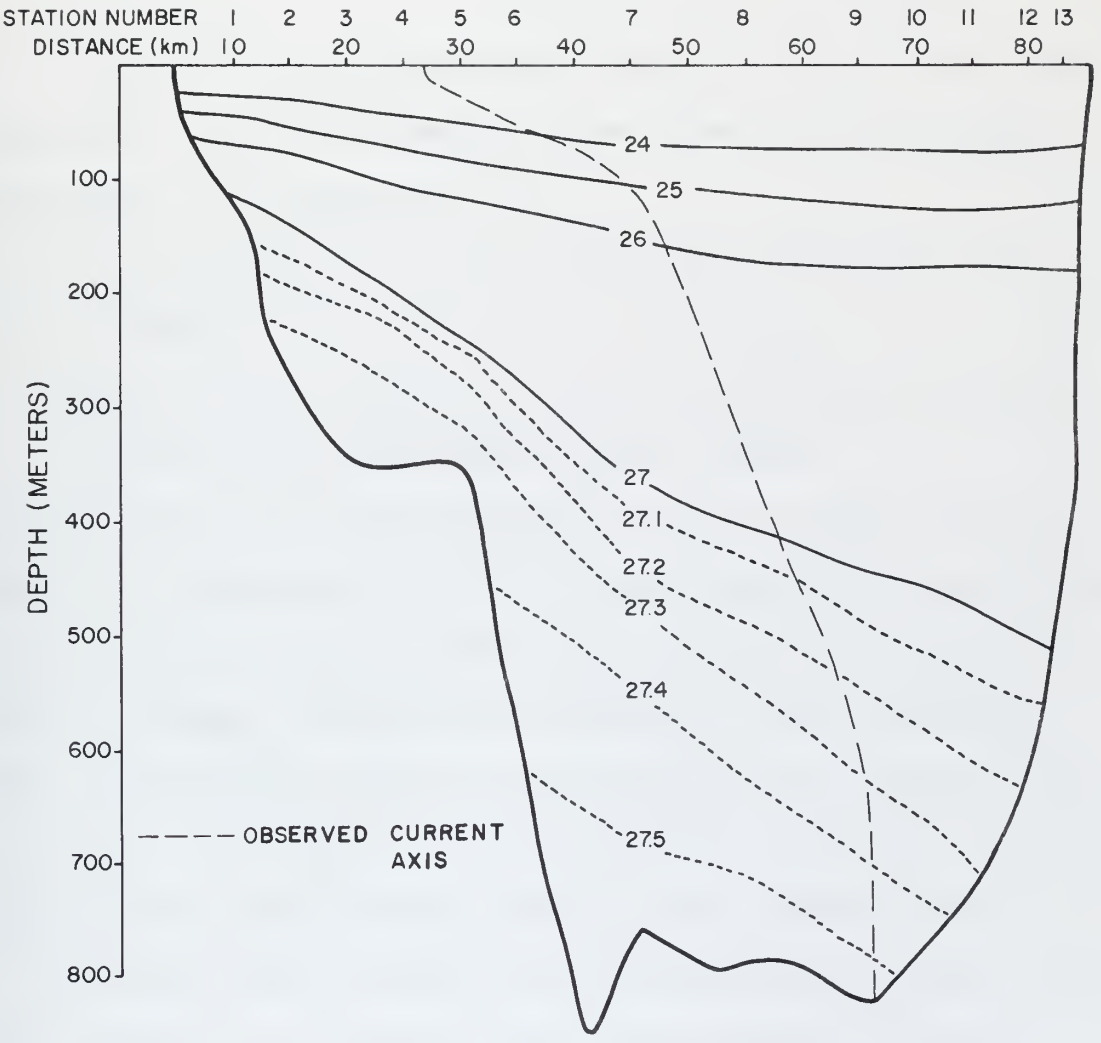

Figure 4. Mean sigma-t section.

transport available at several depths, a transport versus depth curve was drawn for each occupation of each station. Values were read from each curve at 50 meter intervals; these values were then averaged to obtain the mean volume transport curves. By differentiation of these curves, the mean velocity versus depth profiles were obtained.

Using the method of least squares, second, third and fourth order polynomials were fitted to these transport curves. Two constraints were placed on the polynomials:

1. The transport was forced to equal zero at zero depth (sea surface.
2. At zero depth, the derivative of the polynomials was forced to equal the observed mean surface velocity.

An examination of the various orders of polynomials showed that the third order generally had the best fit and resulted in the most realistic profile. The third order polynomial was also used as the best fit in a similar treatment of free-fall data (Richardson, Schmitz and Niiler, 1969). Comparing the velocity versus depth profiles at stations 5 and 7 for second, third and fourth order polynomials (Figure 5), it appears that the third order polynomial yields the most realistic profile.

The methods described above for determining a mean transport curve, and, subsequently, the velocity versus depth profiles, were not the only ones attempted. After several tries, it was found that 50 meters was the minimum increment that could be used for fitting a polynomial to a mean transport curve.

Another method tried was a least squares polynomial fit (with the same two constraints) to the raw transport data, i.e. the actual values

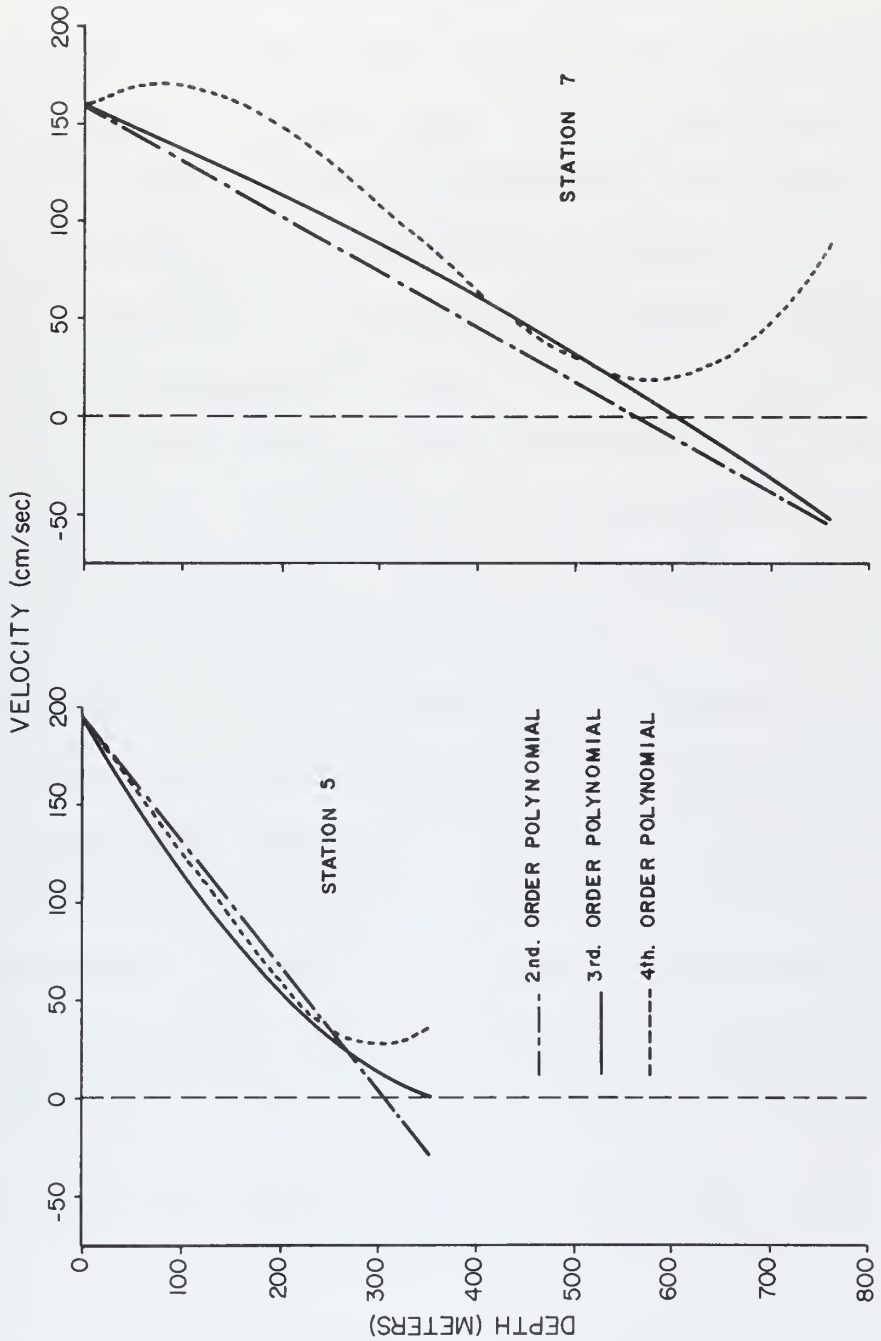

Figure 5. Observed velocity profile for stations 5 and 7.

of transport available at several depths. This method resulted in less realistic velocity profiles, particularly in stations such as 11, 12 and 13 where fewer observations were made.

At a sample station, direct differentiation of the mean transport curve resulted in a velocity profile that was comparable to the one obtained by differentiation of the polynomial. The method used in this thesis cannot be said to be the "best" method, but it does yield velocity profiles that are reasonable when compared with previous works.

The resulting mean axial velocity structure across the Florida Straits is shown in Figure 6. The current axis of this nine day mean velocity field was superimposed on the temperature, salinity and sigma-t sections (Figures 2, 3 and 4). Of particular note is the southward flow near the bottom between stations 2 and 8. This southerly flow, which is discussed in Chapter IV, is in agreement with Wust (1924), bottom photos of ripplemarks by Neumann (1970), and the direct measurements by Düing and Johnson (1971) and Düing (1971).

The geostrophic currents were computed according to the classical dynamic method. As derived by Sandstrom and Helland-Hansen (1903), the relative velocity between two isobaric surfaces, under the assumption of geostrophic flow, can be expressed as

$$v_2 - v_1 = \frac{10}{f\Delta x}\left(\int_{p_1}^{p_2} \alpha_A dp - \int_{p_1}^{p_2} \alpha_B dp\right) \qquad \text{(II-1)}$$

where

f is the vertical component of the Coriolis parameter, $f = 2\omega\sin\phi$ and ω is the angular rotation of the earth and ϕ is the latitude;

Δx is the horizontal distance between stations A and B;

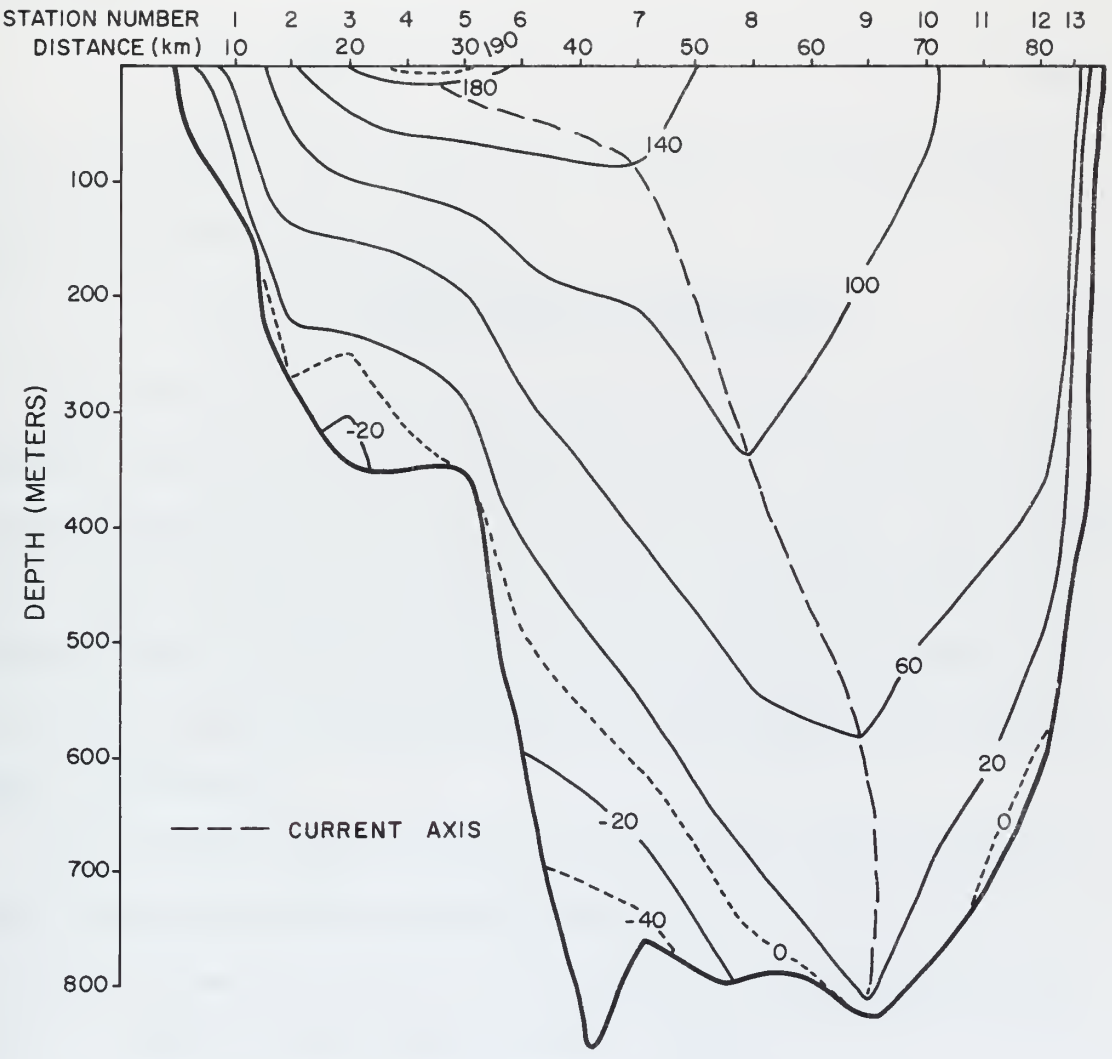

Figure 6. Mean observed axial velocity (cm/sec).

α is the specific volume, $\alpha_{STP} = \alpha_{35,0,p} + \delta$ and δ is the specific volume anomaly;

and, $p_{1,2}$ is the pressure on isobarib surfaces 1 and 2.

The dynamic depth, D, at isobaric surface p_1, referenced to an isobaric surface p_0, is

$$D = \int_{p_0}^{p_1} \alpha dp \qquad \text{(II-2)}$$

By substitution of (II-2) into (II-1), the relative velocity between isobaric surfaces 1 and 2 becomes:

$$v_2 - v_1 = \frac{10}{f} \frac{[(D_2)_A - (D_1)_A] - [(D_2)_B - (D_1)_B]}{\Delta x} \qquad \text{(II-3)}$$

With the field of mass known, (II-3) can be used to compute the relative current field (Neumann and Pierson, 1966). To determine the absolute velocity field, there must be at least one level, the reference level, where the absolute velocity is known. The establishment of a reference level is usually difficult and speculative. Computation of the absolute velocity field is possible if good quality direct measurements are available.

The following direct and indirect methods were used to determine the reference level across the Florida Straits:

(1) Determination from the observed data of the depth where the observed velocity equals zero. (direct)

(2) Setting the observed and computed velocities equal at the surface. (direct)

(3) Defant's ΔD method. (indirect)

The depth of no motion is the depth where the mean current component normal to the section is zero. The use of direct measurements to

determine the depth of no motion is best suited to a region where the mean current is strong. The observed velocity versus depth curves yields the depth of no motion, if one exists, for each station. Knowing the depth of no motion, the absolute velocity field can be computed.

Alternatively, the directly measured surface current can be used to convert the relative velocity field into an absolute one. A reference level results by setting the geostrophic surface velocity equal to the observed surface velocity. On the anticyclonic side, equating the two surface velocities did not indicate a depth of no motion in some cases, i.e. northward flow filled the entire water column.[3]

For strongly stratified fluids, one of the most reliable indirect methods is that proposed by Defant (1941). The Defant method consists of comparing relative dynamic depth differences at given isobaric surfaces between two stations and to determine at what level the dynamic depth difference is constant. This process defines a level with a constant horizontal pressure gradient, which is hypothesized to be the depth of no motion.

The differences in the dynamic depths, computed relative to the sea surface, were compared for various combinations of station pairs. In the majority of the comparisons there was a definite layer where ΔD was constant. Near the boundary on the anticyclonic side, several of the comparisons did not show a distinct level of constant ΔD. Figure 7 shows typical ΔD profiles for the cyclonic side, the middle, and the anticyclonic side of the Florida Current. For these profiles

---

[3]Anticyclonic side in the Florida Current is where the relative vorticity is negative, i.e. the eastern side. The cyclonic side is where the relative vorticity is positive, i.e. the western side.

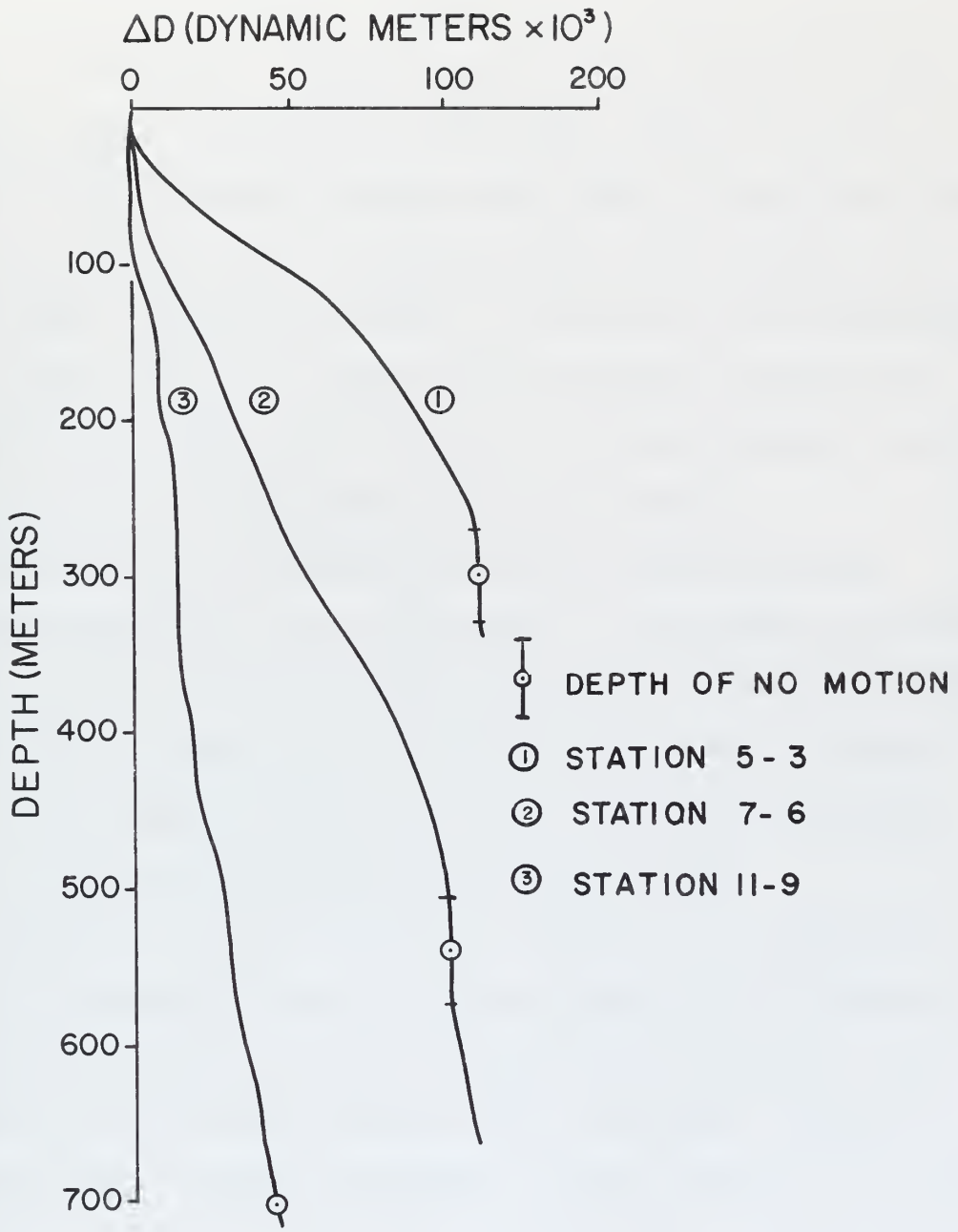

Figure 7. Mean dynamic depth difference (ΔD).

the layers over which ΔD is constant are 60, 70 and 5 meters respectively.

Using the three methods outlined above, a section showing the depth of no motion was computed (Figure 8). The extension of the reference level from method (2), $\bar{V}$geostrophic = $\bar{V}$observed at the surface, into the eastern boundary occurs where northward flow filled the entire water column. The doubtful areas of the reference level from method (3), the Defant method, are indicated by dots superimposed on the solid line. It is clear that the differences between these methods are not great. Typically it is a 25 meter difference west of station 8 and a 50 meter difference east of station 8.

Different geostrophic calculations were made using various reference depths and various station pairs. In some cases the reference depth was below the maximum depth of one of the stations due to sloping boundaries. In these cases it was necessary to extend the dynamic calculations below the bottom. For these calculations, the dynamic depth profile was extrapolated to the necessary depth.

Downstream velocity sections were computed using a depth of no motion as determined by Defant's method (Figure 9) and by matching of observed and computed velocities at the surface (Figure 10). Both figures have the observed velocity field superimposed. Compared to the geostrophic isotachs, the observed isotachs, except near the surface, are deeper and skewed to the east. In both figures, the best agreement between observed and geostrophic occurs on the cyclonic side.

Two additional indirect methods are shown in Figures 11 and 12. A velocity section was computed using the bottom as the depth of no motion and compared with the observed field (Figure 11). The

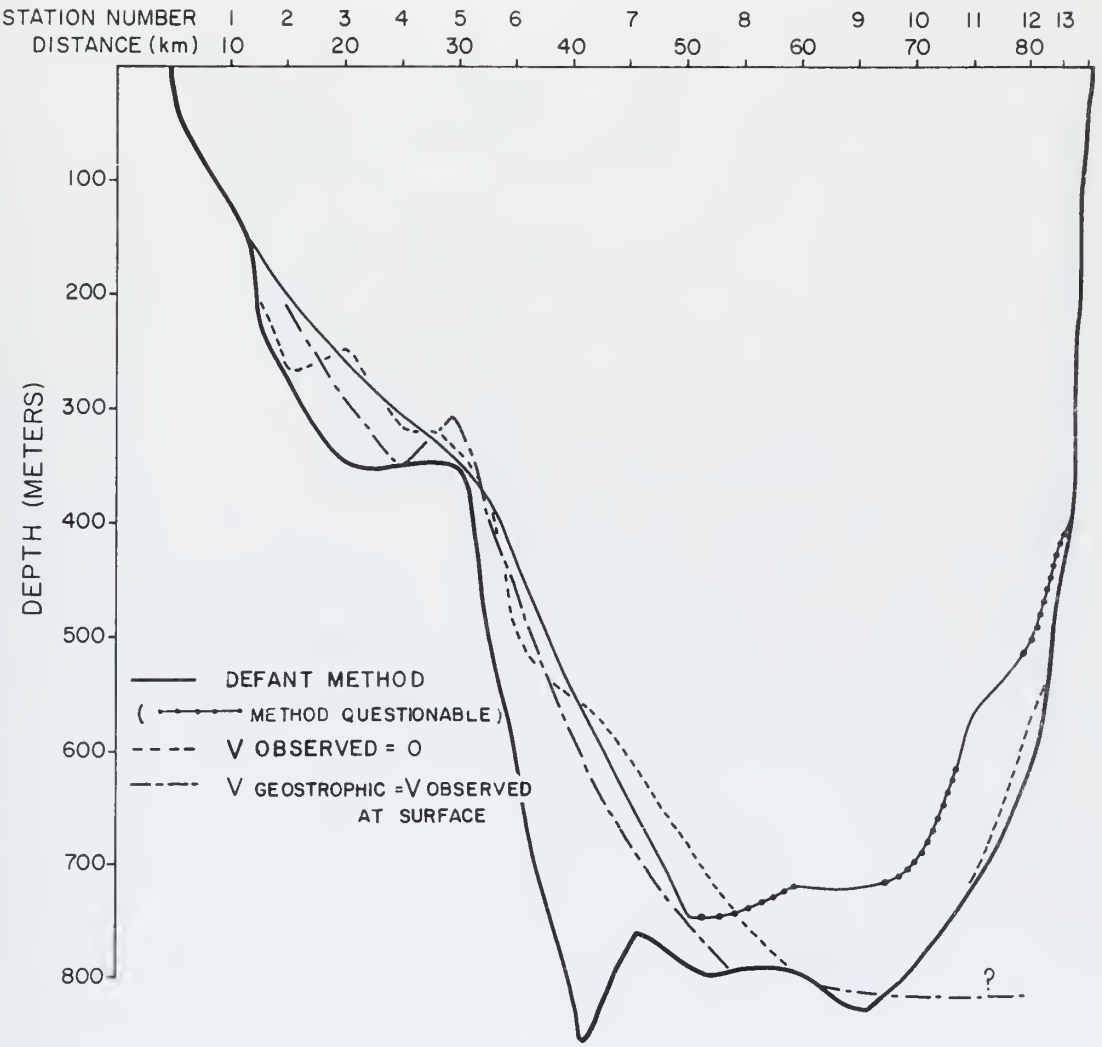

Figure 8. Depth of no motion.

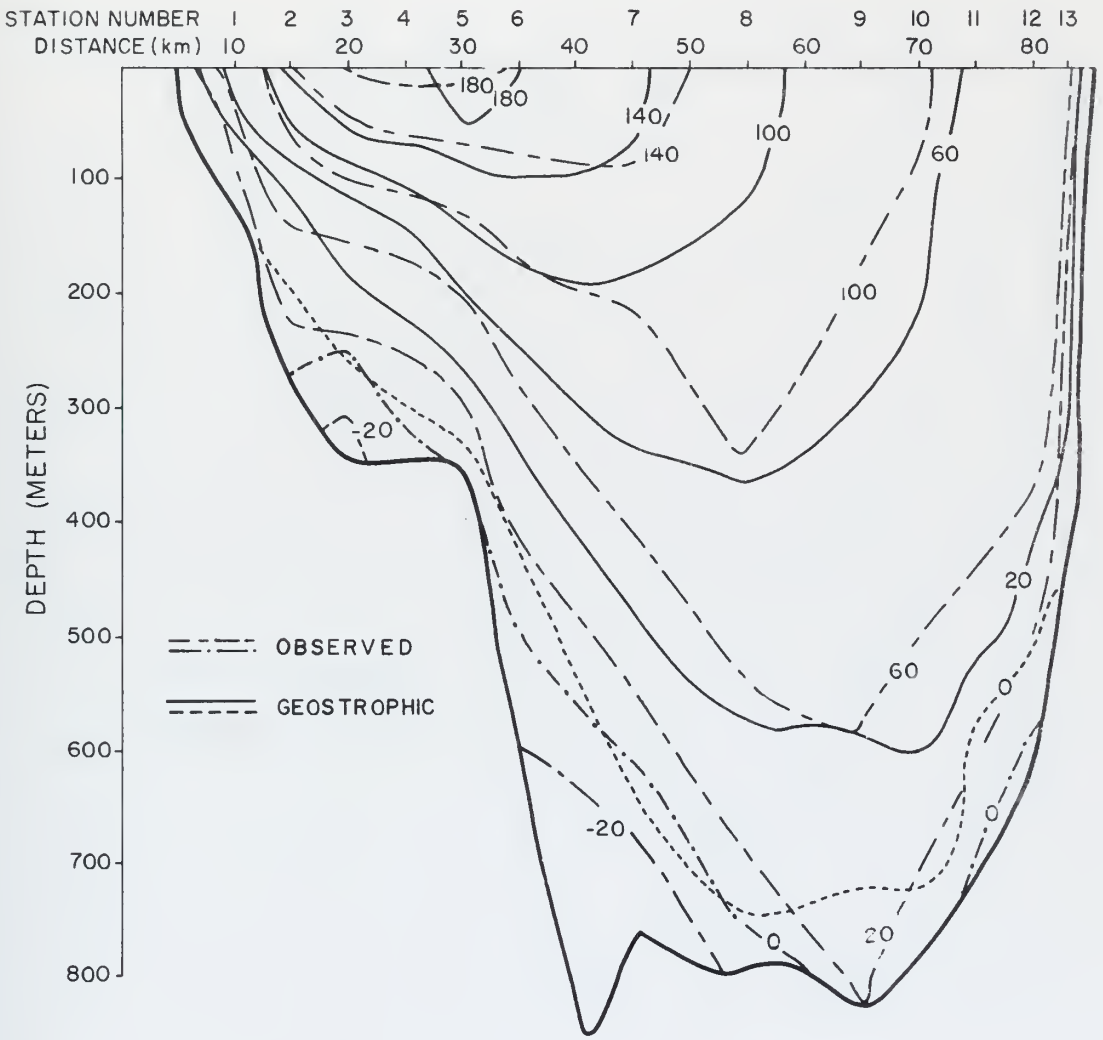

Figure 9. Mean axial velocity (cm/sec), observed and geostrophic (depth of no motion by Defant's method).

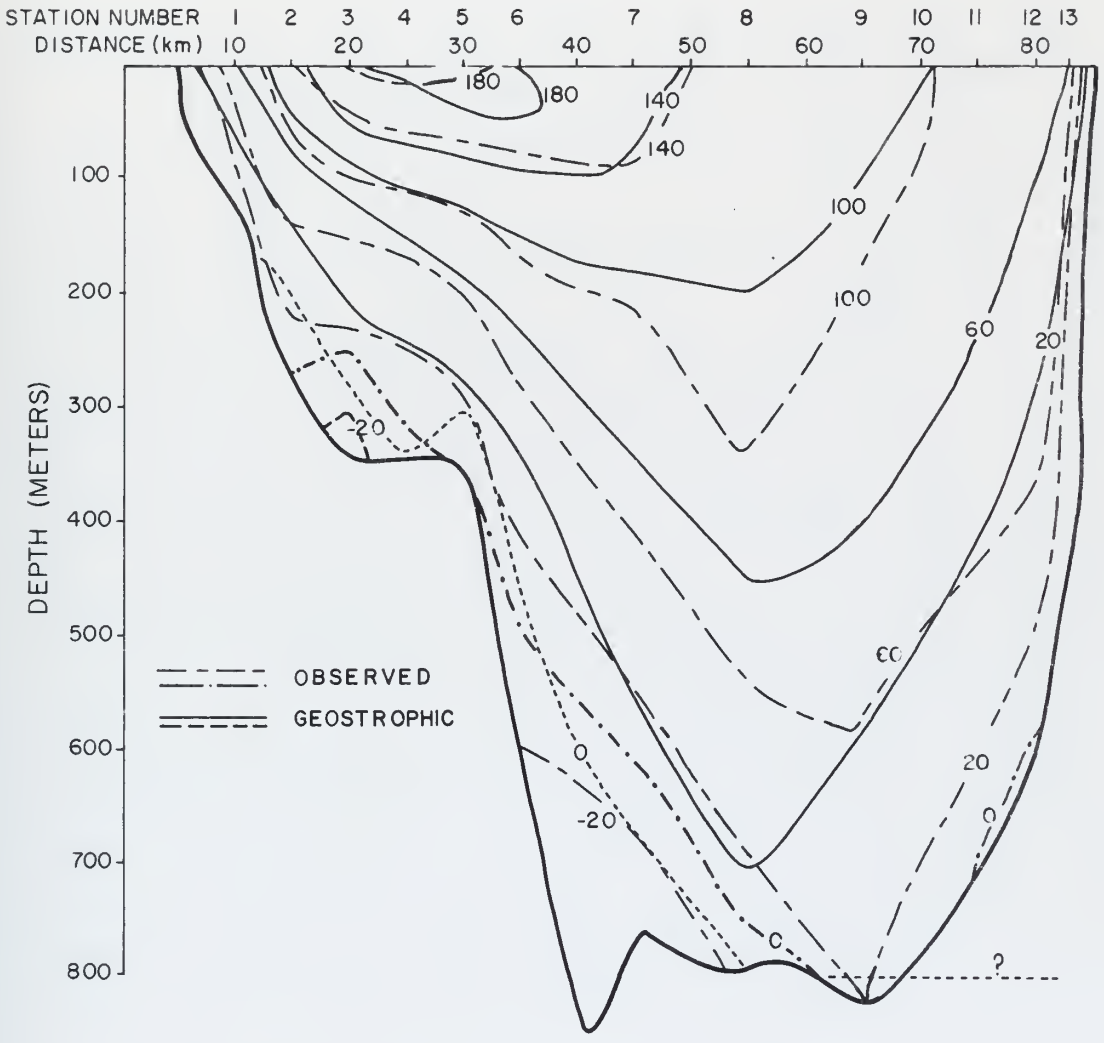

Figure 10. Mean axial velocity (cm/sec), observed and geostrophic ($V_{geostrophic} = V_{observed}$ at surface).

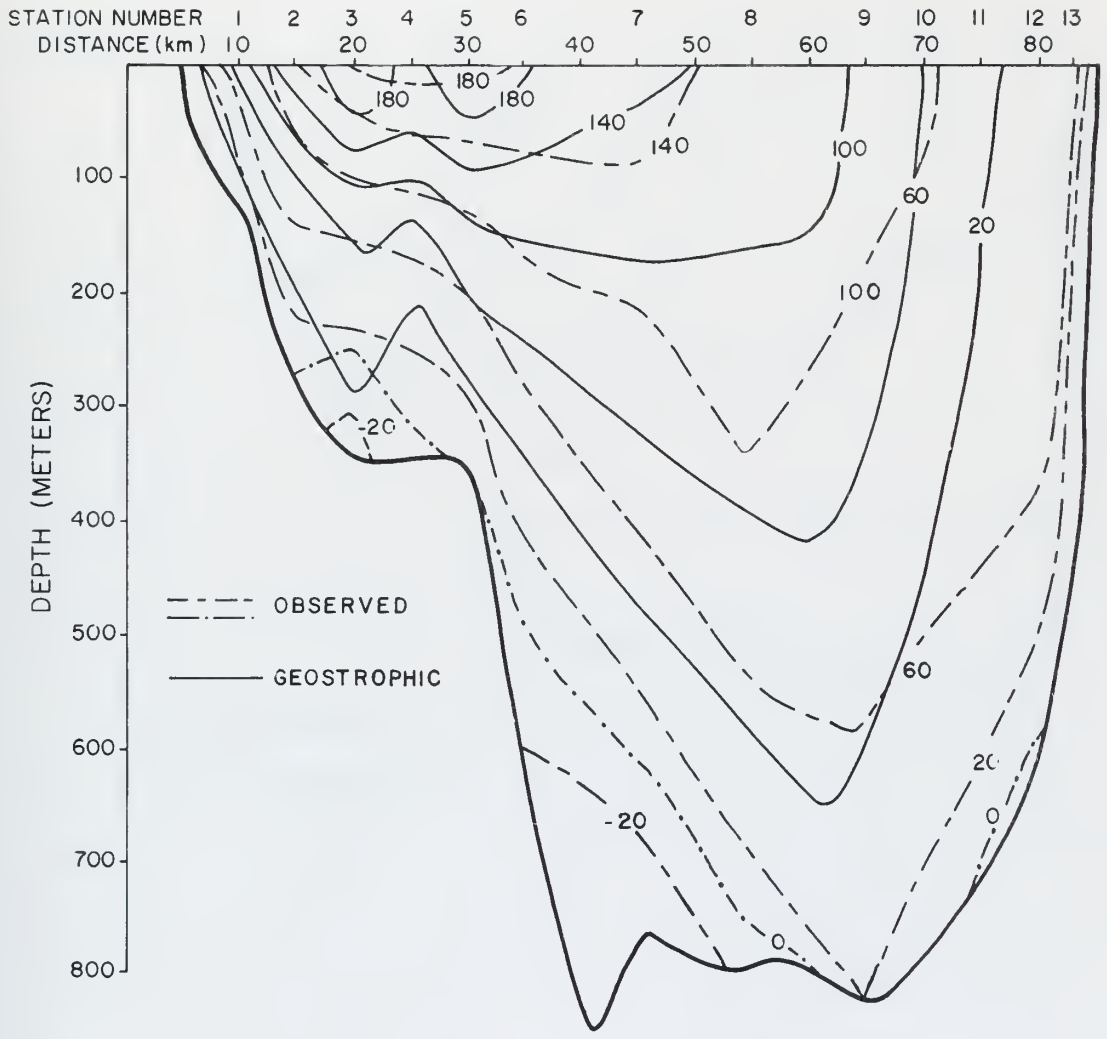

Figure 11. Mean axial velocity (cm/sec), observed and geostrophic ($V_{geostrophic}$ = 0 at bottom).

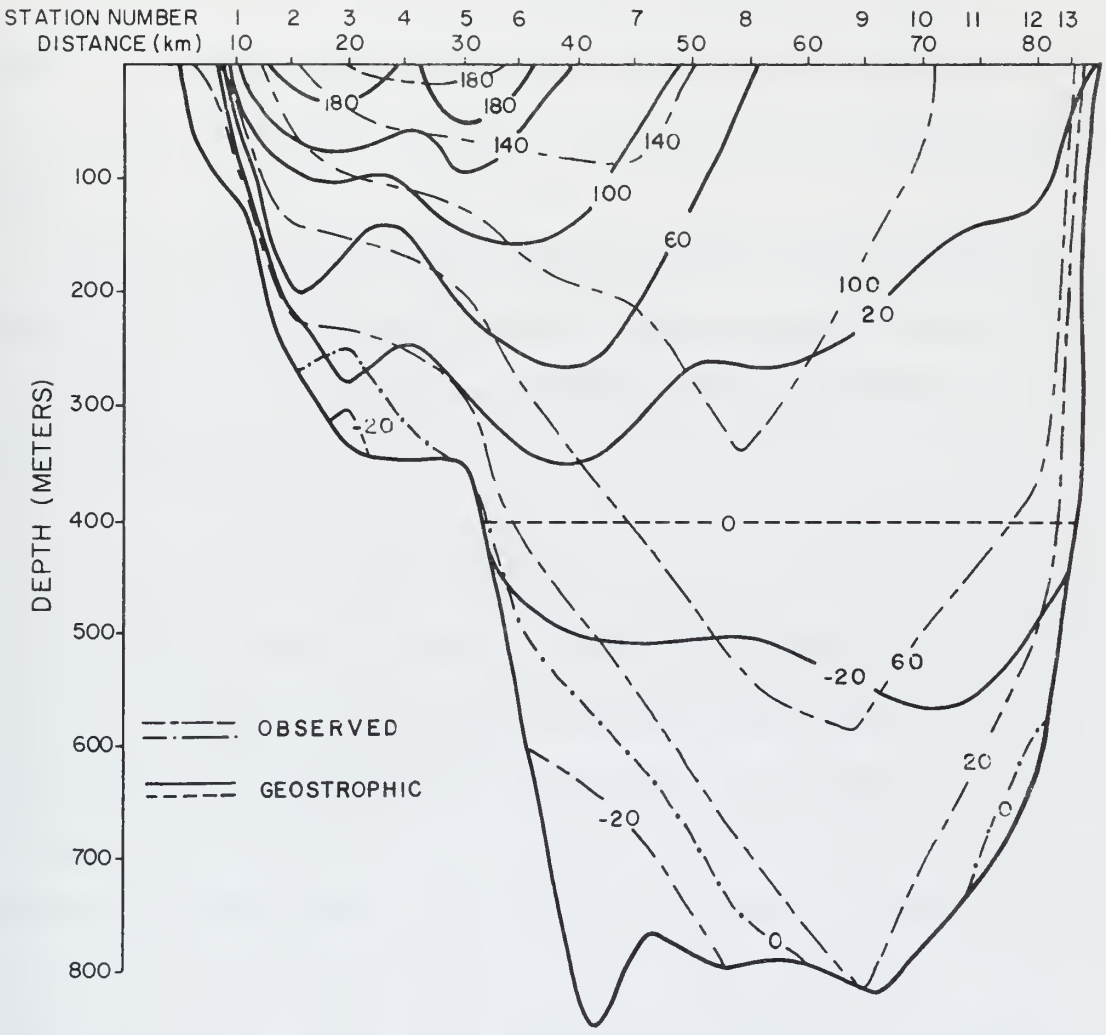

Figure 12. Mean axial velocity (cm/sec), observed and geostrophic (depth of no motion = 400 meters).

biaxial structure is similar to the results of Broida (1966). Broida's biaxial structure was attributed to internal tidal aliasing. In this case the structure is due to the use of a non-realistic depth of no motion on the cyclonic side.

To illustrate the effect of a constant depth of no motion, a section was computed using 400 meters as the depth of no motion (Figure 12). Again the biaxial structure is a result of an unrealistic reference depth.

In each of the geostrophic sections computed, the following combinations of station numbers were used: 1-3, 2-4, 3-5, 4-6, 6-8, 7-9, 9-11 and 10-12. All isotachs were extrapolated to the boundary at the surface or interior.

C. ERRORS

The errors associated with the free-fall instrument data have two sources: the system errors and the possible interpretative errors arising from the assumptions that conditions are stationary over the time and space scales of a run. The system error consists of navigational and timing errors. The Hifix has an error of ± 1 meter on the western side of the Straits and ± 2 meters on the eastern side. The timing error is ± 1 second. The system error yields an error estimate for the surface velocity of $\pm 3\%$ and for the transport of $\pm 5\%$ (Richardson and Schmitz, 1965). For the short run time (1-10 minutes) and the short horizontal distance of a run (10-500 meters), experience has demonstrated that fluctuations large compared to the mean axial flow do not occur over these scales in the Florida Current.

A transect is completed in about 8 hours. As stated previously, mean values vice daily values were used to reduce the effect of tidal aliasing. In addition, the station times were varied as much as practicable to reduce tidal aliasing. Examination of the times of station occupation over the nine day period (Table II) reveals that there is little variation in those times for the stations in the middle of the Straits. The diurnal tidal motion may therefore have a greater aliasing than the semi-diurnal. Furthermore, the solar diurnal may have a greater aliasing effect than the lunar diurnal.

Using the times of station occupation and values of the various tidal harmonic constants from Florida Current data (Smith, Zetler and Broida, 1969), the tidal aliasing error in the observed velocities is $\pm$3% for the axial velocity. The error is approximately 25% for the cross-stream velocity. Appendix A gives the procedure used to calculate these errors.

The values of depth, temperature and salinity were read directly from the STD trace within the limits:

depth, $\pm$0.5 meters;

temperature, $\pm$0.025°; and

salinity, $\pm$0.05‰ .

The geostrophic velocity error is a sum of the relative errors in depth, horizontal separation, and density. The relative error in the density of $\pm$20% is more than one order of magnitude greater than the relative errors in depth and horizontal separation. Hence, the relative geostrophic velocity error is $\pm$20%.

A comparison of σ_t and $\rho_{in\text{-}situ}$ at the deepest station, number 10,

showed that the approximation of the density field by σ_t resulted in negligible error.

For an indication of the variability of the data, the standard deviations for temperature, salinity and sigma-t are plotted (Figure 13). The area of maximum variance in these parameters is in the pycnocline on the cyclonic side.

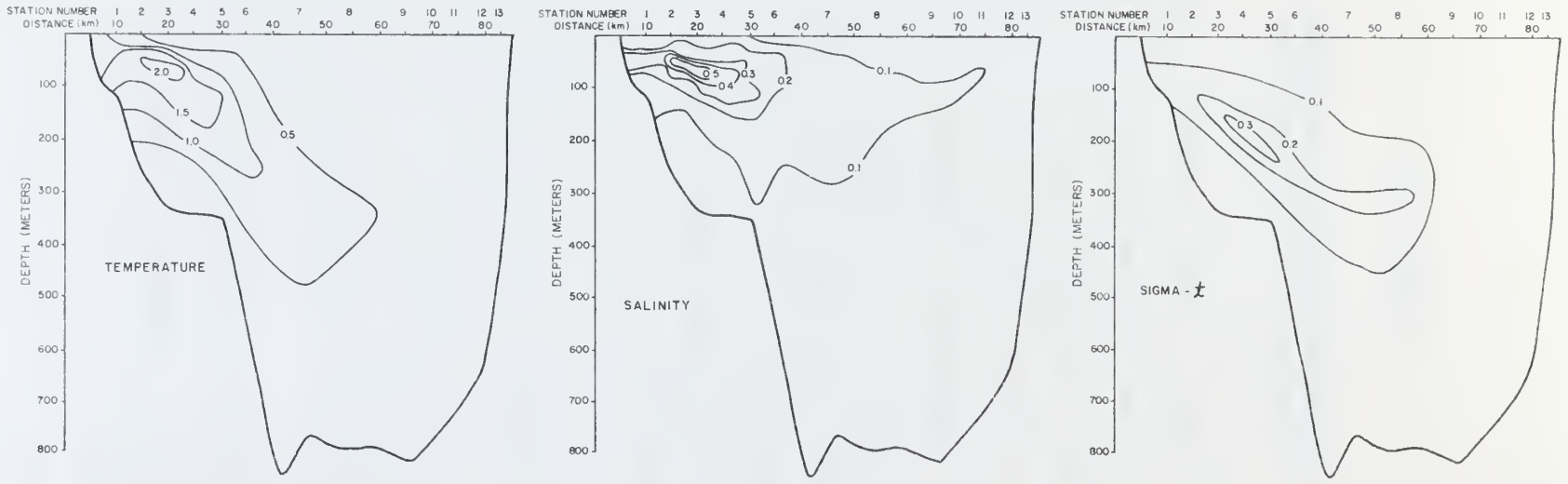

Figure 13. Standard deviation for temperature (C^{o}), salinity (‰), and sigma-t (σ_t units).

III. RESULTS

A. COMPARISON OF DIRECT MEASUREMENTS WITH GEOSTROPHIC MEASUREMENTS

Other than on the anticyclonic side, where the Defant method is in doubt, there is a good agreement between the directly and indirectly determined depths on no motion (Figure 6). From this figure, a "best" depth of no motion, called a hybrid depth of no motion, is chosen and used for the final comparisons of observed and computed fields. On the cyclonic side, the hybrid depth of no motion is the level determined by the Defant method. On the anticyclonic side, it is the bottom. Since the hybrid depth of no motion nearly coincided with the depth where the observed velocity equals zero, the latter could have been used as the best depth of no motion. The hybrid depth was chosen for the following reasons:

(1) it does closely approximate the depth of no motion determined by the observed velocity field, and

(2) its use sets a precedence for determining a depth of no motion in the Florida Straits when no observed velocity data are available.

The computed surface velocity distribution using both the Defant and hybrid reference depths is compared to the observed surface velocity distribution in Figure 14. On the anticyclonic side the agreement between computed and observed surface velocities is poorer than on the cyclonic side. East of station 9, the surface velocities computed with

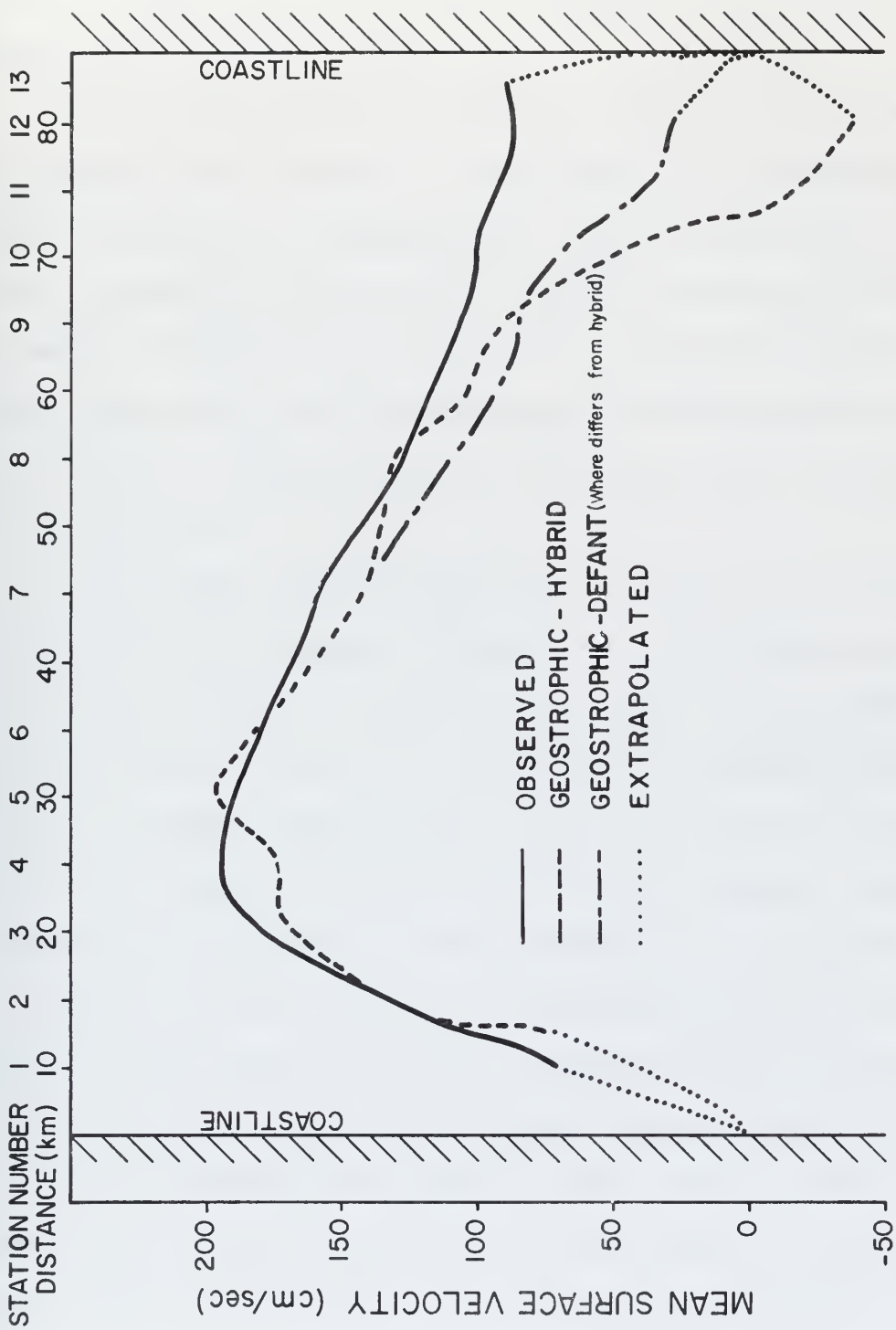

Figure 14. Mean surface velocity (cm/sec), observed and geostrophic (hybrid depth of no motion).

the hybrid depth shows less agreement with the observed surface velocities than those computed using the seemingly less reliable depth found by Defant's method.

Using the hybrid depth of no motion, a comparison of the computed and observed velocity sections is made (Figure 15). As with the surface velocities, the best agreement is on the cyclonic side of the stream. Compared to the geostrophic velocity, the observed isotachs are deeper, except near the surface, and the observed current axis is skewed to the east. The agreement between the position of the observed current axis and the position of the geostrophic current axis improves as depth increases.

The geostrophic, using the hybrid depth of no motion, and observed velocity profiles are compared in Figure 16 for each station where both computed and observed values were available. The geostrophic subsurface maximum at station 11 is similar to the observed subsurface maximum by Düing and Johnson (1971). The closest fit of the absolute values of the curves occurs on the cyclonic side. However, comparison of the vertical shear shows the best agreement on the anticyclonic side.

Because of the uncertainties in determining the observed velocity fields by differentiation of the mean transport curves, an informative, if not more accurate, test of the validity of the geostrophic approximation is the comparison of transport curves. Figure 17 shows transport per unit width curves, observed and computed. A representative station from the cyclonic side, the middle and the anticyclonic side is used for the comparison. The previously established pattern of close agreement of absolute values on the cyclonic side and poorer agreement

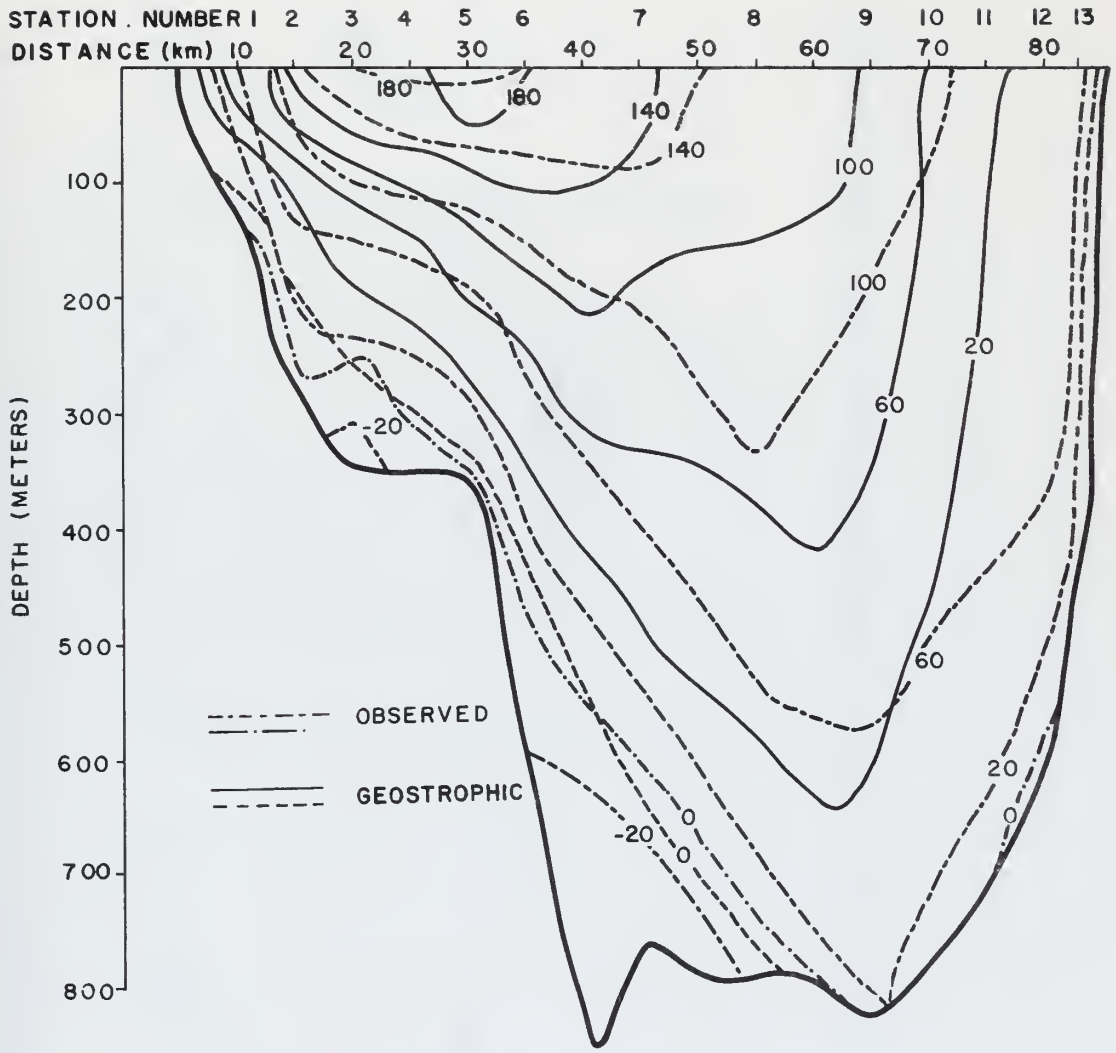

Figure 15. Mean axial velocity (cm/sec), observed and geostrophic (hybrid depth of no motion).

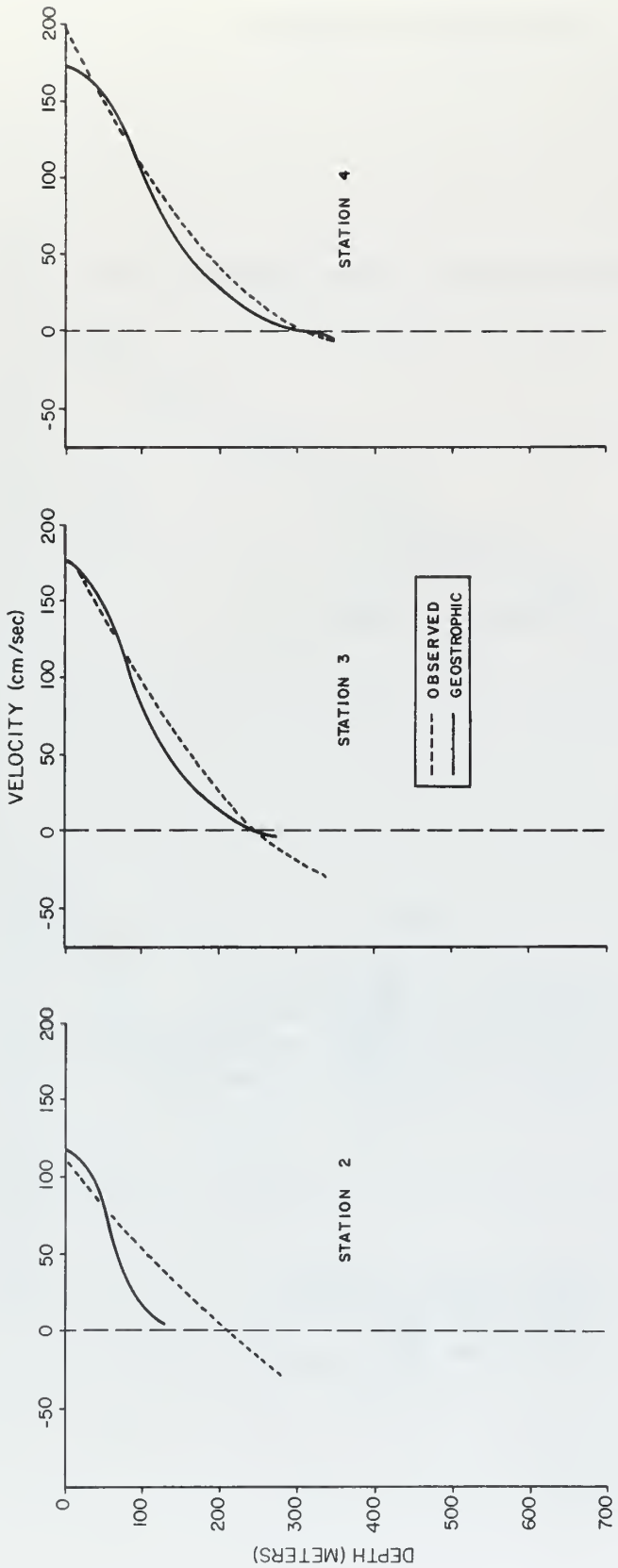

Figure 16a. Velocity profile (cm/sec), observed and geostrophic (hybrid depth of no motion), stations 2, 3 and 4.

THE UNIVERSITY OF MIAMI

The Baroclinic Structure of the Florida Current

BY

William O. Stubbs, Jr.

A THESIS

Submitted to the Faculty
of the University of Miami
in partial fulfillment of the requirements for
the degree of Master of Science

Coral Gables, Florida

June 1971

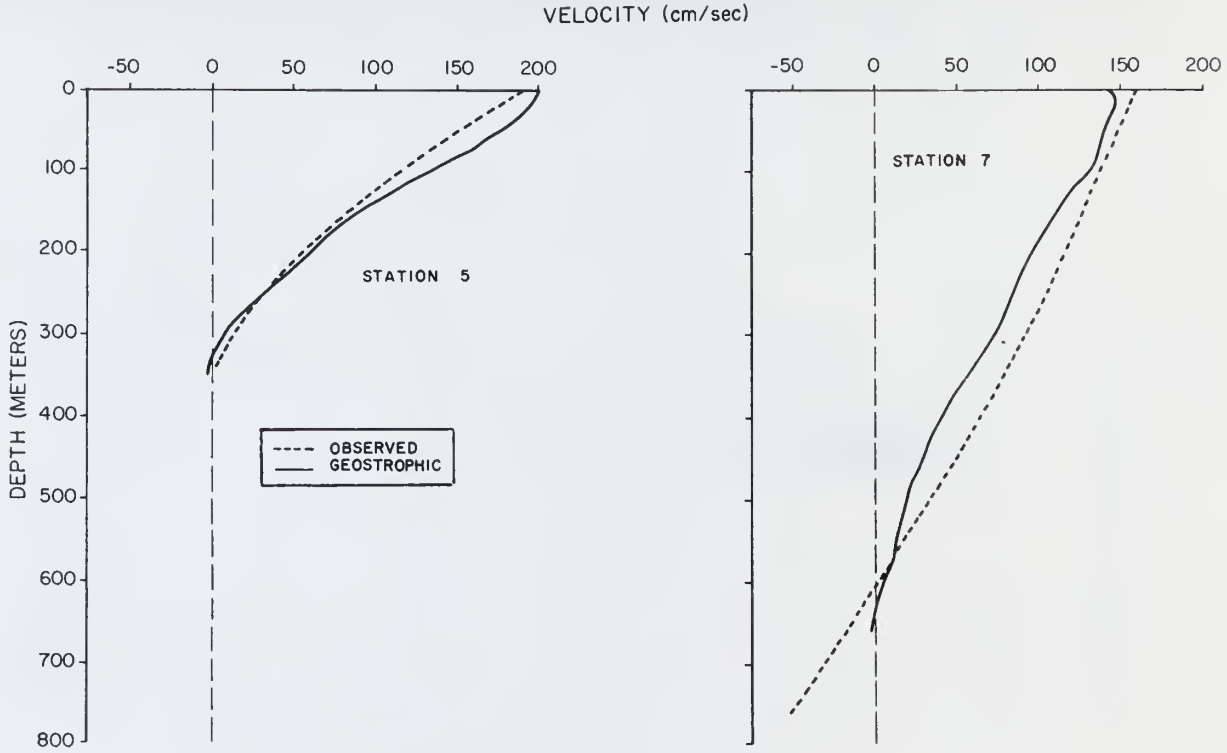

Figure 16b. Velocity profile (cm/sec), observed and geostrophic (hybrid depth of no motion), stations 5 and 7.

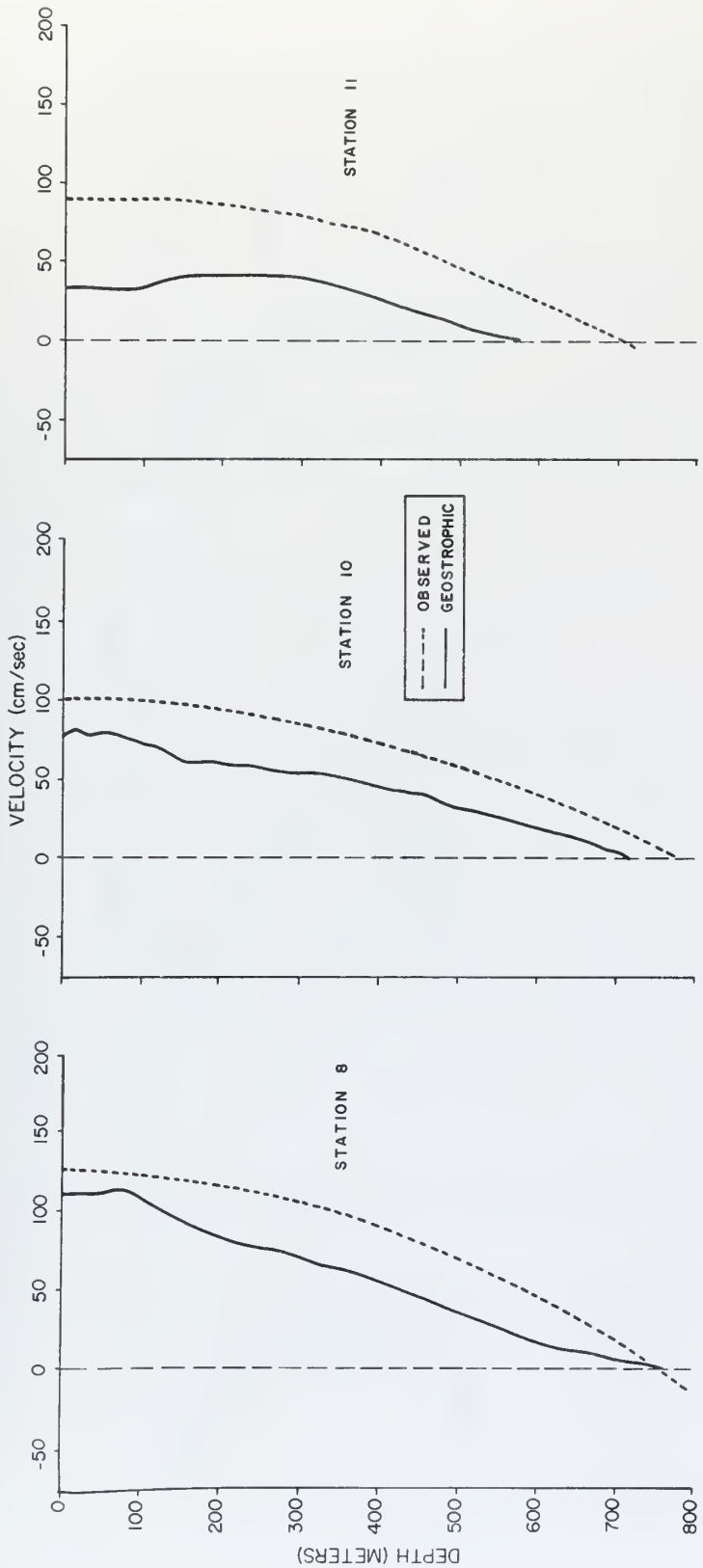

Figure 16c. Velocity profile (cm/sec), observed and geostrophic (hybrid depth of no motion), stations 8, 10 and 11.

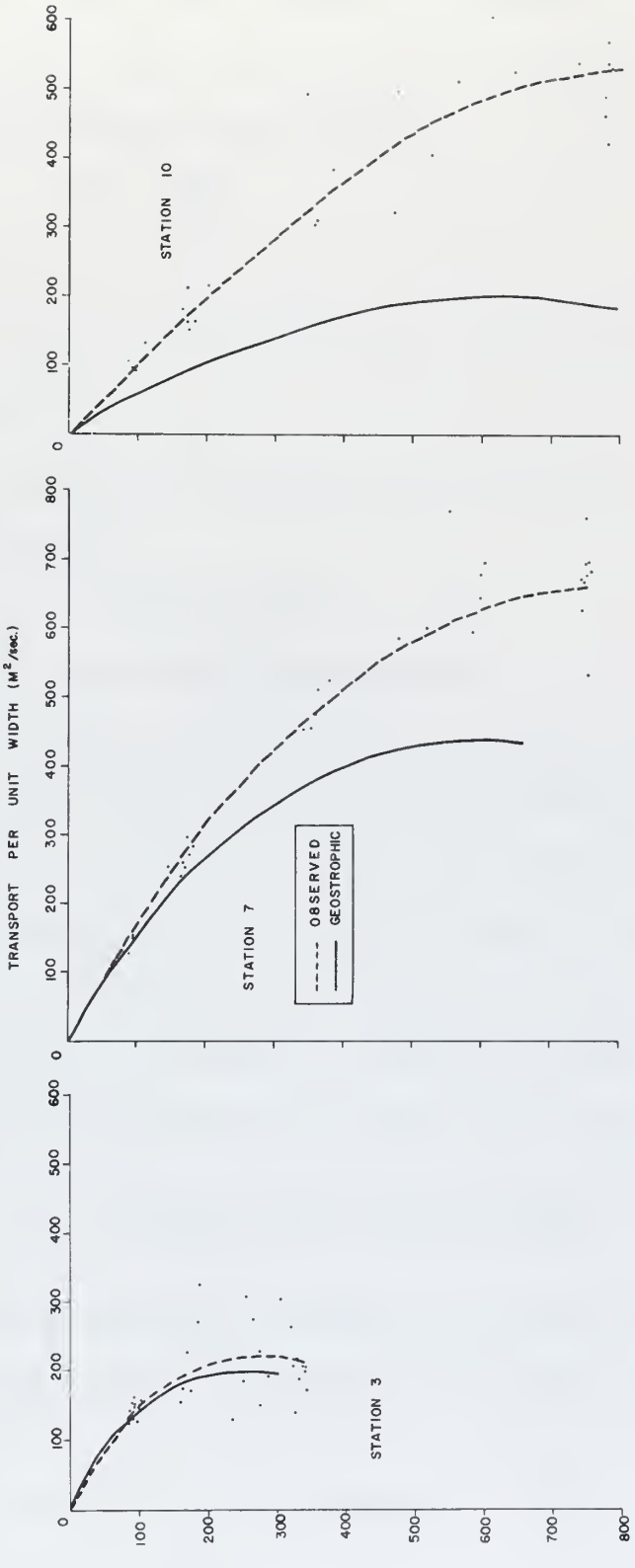

Figure 17. Transport per unit width (m^2/sec), observed and geostrophic (hybrid depth of no motion), stations 3, 7 and 10. Dots indicate free-fall data.

on the anticyclonic side is clearly illustrated.

The thermal wind relation derived from the assumption of geostrophic and hydrostatic equilibrium is

$$f\bar{v}_z = -\frac{\bar{\rho}_x g}{\rho_o}$$

where

$\bar{v}_z$ is the derivative with respect to depth of the mean axial velocity,

$\bar{\rho}_x$ is the derivative with respect to horizontal distance of the mean density,

ρ_o is the reference density,

and, g is the gravitational acceleration.

Using the observed velocity and density data, the ratio of left hand side to the right hand side describes whether or not the thermal wind relation is satisfied. If the ratio is unity, the thermal wind relation is satisfied. If the ratio is greater (less) than one, the observed shear is greater (less) than the geostrophic shear.

From Figure 18, the areas of observed southward flow and the area east of station 9 are where this ratio differs the greatest from unity.

B. FEATURES OF THE FLORIDA CURRENT

To extract additional information about the baroclinic structure of the Florida Current, the free-fall data were analyzed by studying the following:

(1) Baroclinic stability parameter

(2) Richardson number

(3) Mean T-S curves

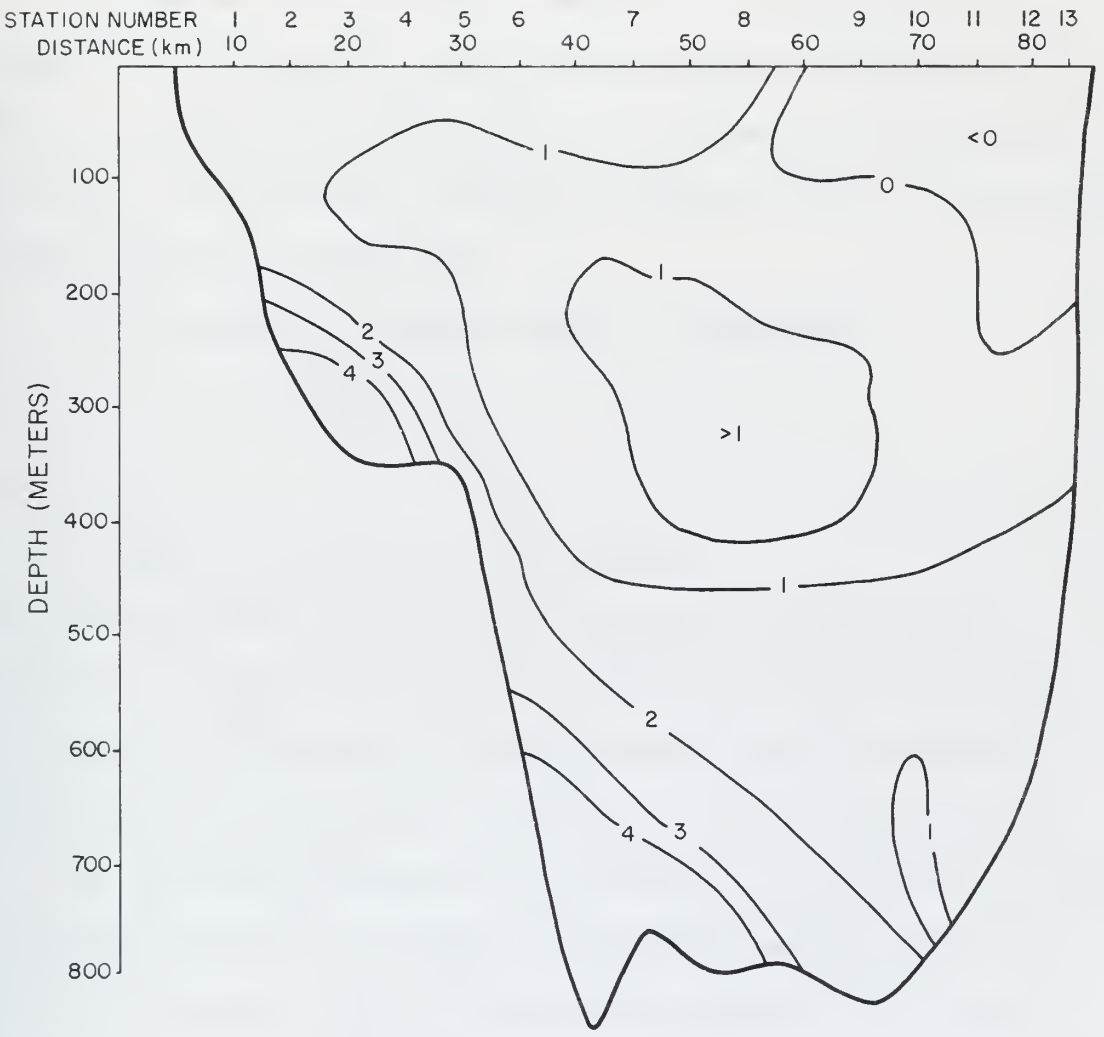

Figure 18. Thermal wind ratio section.

(4) Net transport between selected isopycnals

(5) Total downstream transport

(6) Cross-stream flow

The results of these studies are discussed below.

(1) The baroclinic stability parameter is the ratio of the slopes of an isopycnal, S, to its critical value, Sc (Mooers, 1971). When $S > Sc$, baroclinic instability, or hydrodynamic disequilibrium, can occur. The baroclinic stability is relatively low in the pycnocline on the cyclonic side (Figure 19).

(2) The gradient Richardson number is expressed as

$$Ri = \frac{N^2}{(\overline{v}_z)^2}$$

where

$N^2 = \frac{\overline{\rho}_z}{\rho_o} g$ is the Vaisala-Brunt frequency.

$Ri<1$ implies dynamic instability for the flow, and $Ri>1$ implies stability. From Figure 20, the area where the dynamic stability is the lowest is near the bottom on the cyclonic side. The dynamic stability is the greatest near the surface on the anticyclonic side.

(3) The mean T-S diagrams for stations 2, 6 and 10 (Figure 21) are in agreement with the T-S diagrams presented by Wennekens (1959) for the Florida Current. The cross channel distribution of water mass properties described by Wennekens is illustrated in the T-S curves. Station 2 is representative of the Continental Edge Water, station 6 is representative of the Transition Zone Water, and station 10 is representative of the Yucatan Water. The Yucatan, or Caribbean, Water is identified by its well defined salinity maximum. The great reduction in the intensity of this salinity maximum is the conspicuous feature of

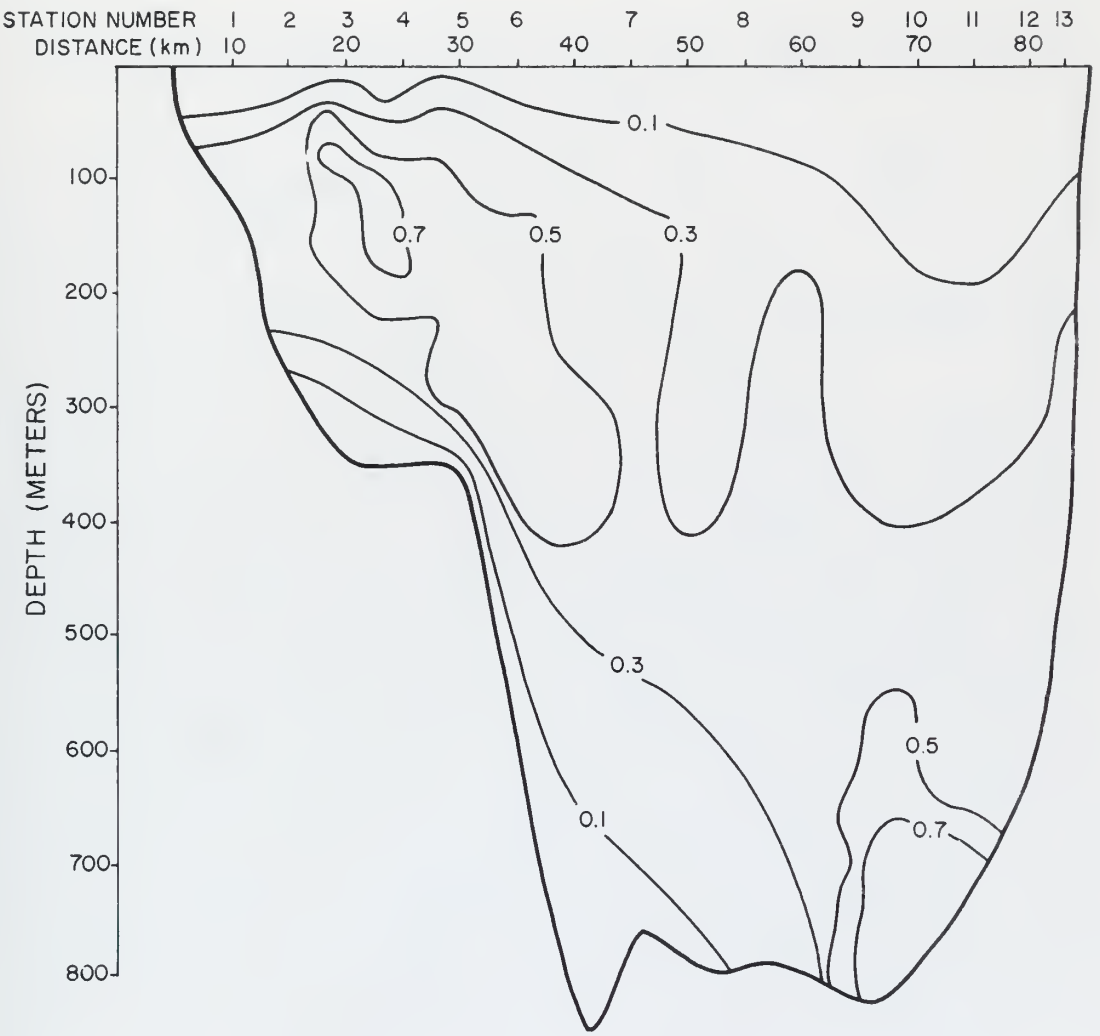

Figure 19. Baroclinic stability parameter section.

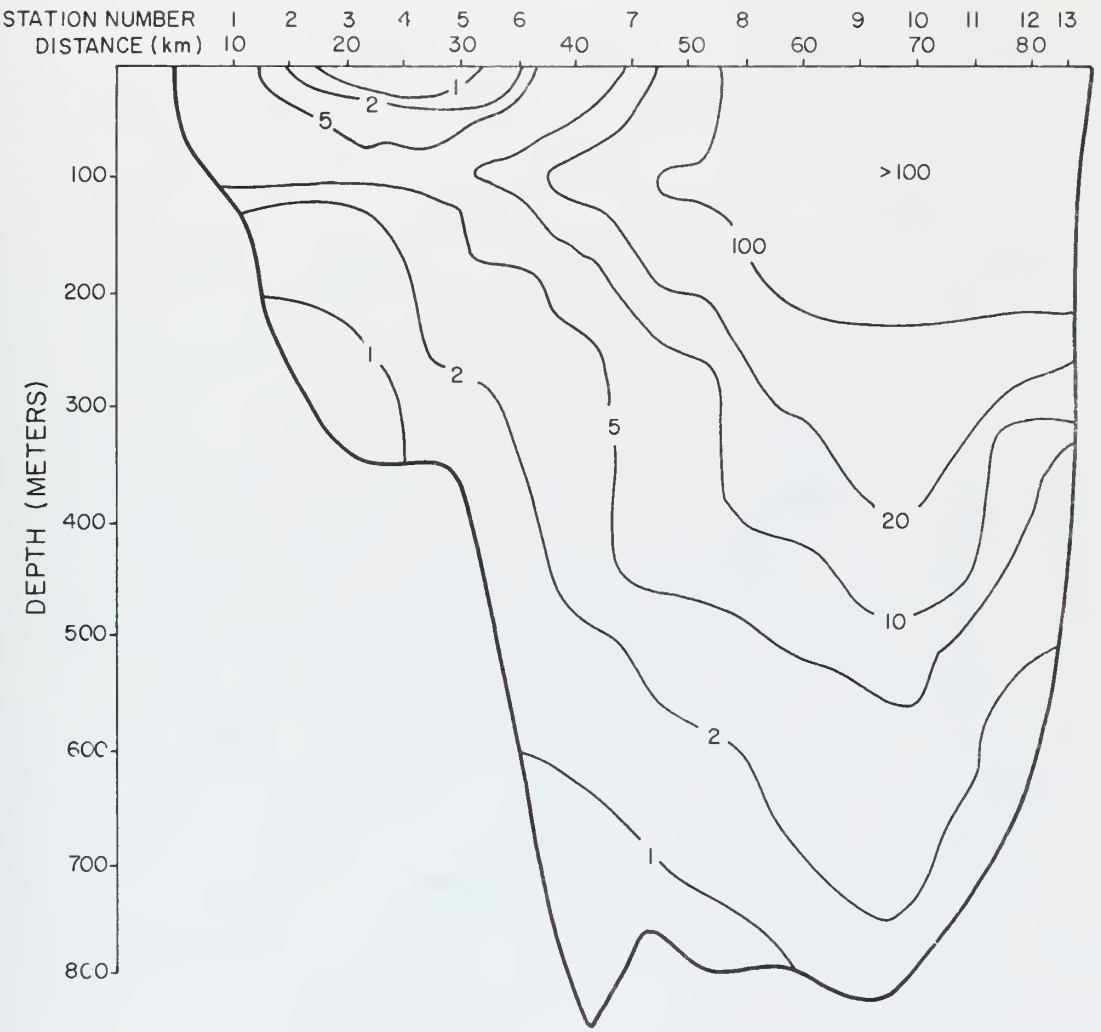

Figure 20. Richardson number section (isolines have non-uniform spacing).

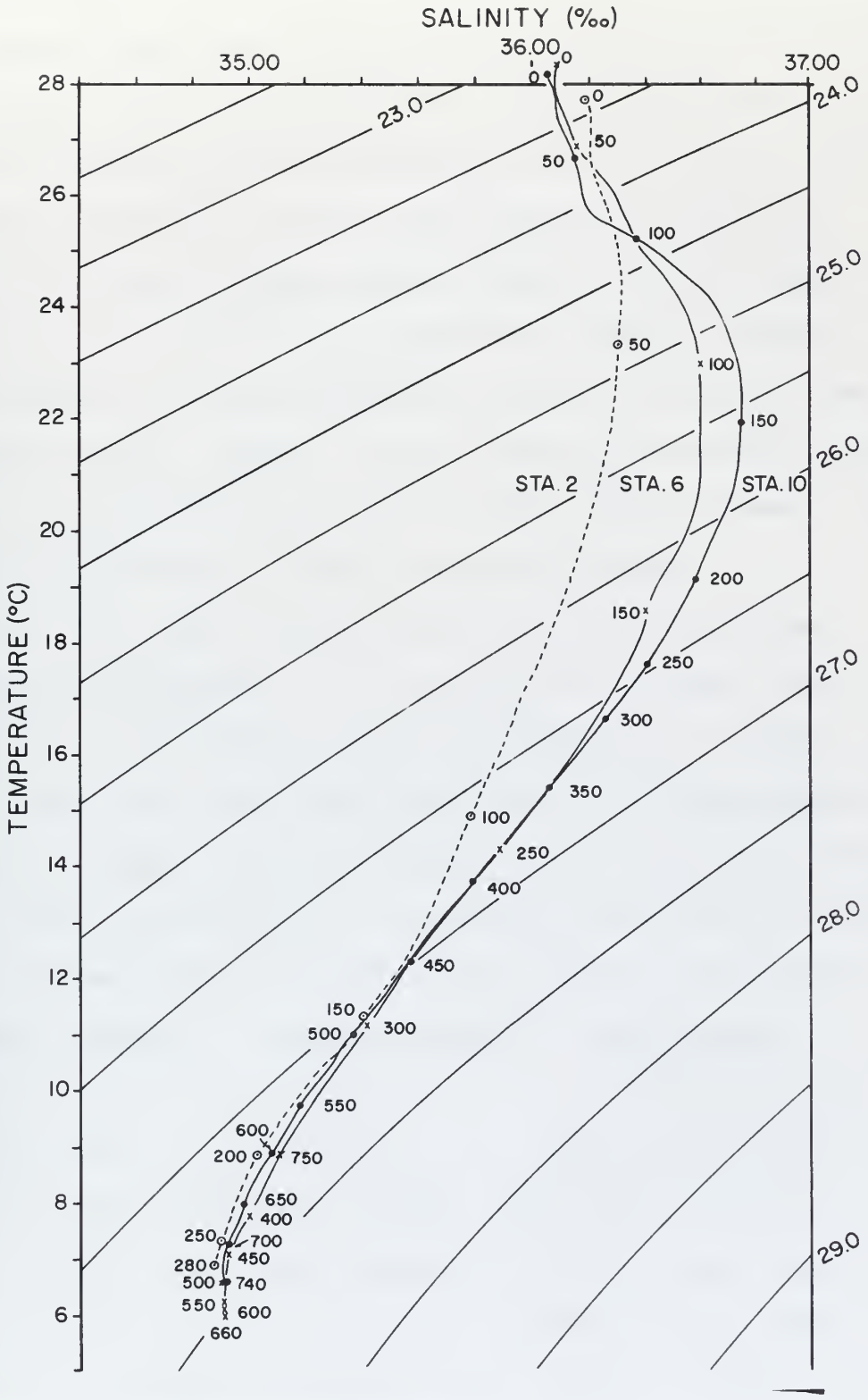

Figure 21. T-S curve, stations 2, 6 and 10.

the Edge Water.

The water that flows through the Florida Straits originally comes, in large part, from the southern half of the North Equatorial Current and from a branch of the South Equatorial Current. This water flows through the Caribbean, and then, without mixing with the waters endemic to the Gulf of Mexico, passes through the Florida Straits in very nearly its original state. Because this water has acquired a large admixture of Antarctic Intermediate Water at mid-depths from the South Atlantic, there is a salinity minimum (between 600 and 800 m depth) in the water exiting out of the Florida Straits (Stommel, 1966). This salinity minimum is present in stations 6 and 10.

(4) The net axial transport across the Straits and between isopycnals was determined in the vicinity of the southward flow. A net transport southward would favor the existence of a southward undercurrent rather than a large scale eddy. In all combinations of isopycnals, the net transport was always greater to the north. This result admits the possibility of a large scale eddy being the cause of the southward flow. An example of the results are shown below.

Isopycnal Interval	Inclusive Stations	Net Transport
27.2 - 27.3	2 - 9	7.5×10^6 m^3/sec North
27.4 - 27.5	6 - 9	3×10^6 m^3/sec North

(5) The net downstream transport value at each station was integrated across the channel (Figure 22). The total mean volume transport of 33.4×10^6 m^3/sec compares favorably with the value obtained by Richardson and Schmitz (1968) of 32.2×10^6 m^3/sec for data averaged over the period of May-June 1965.

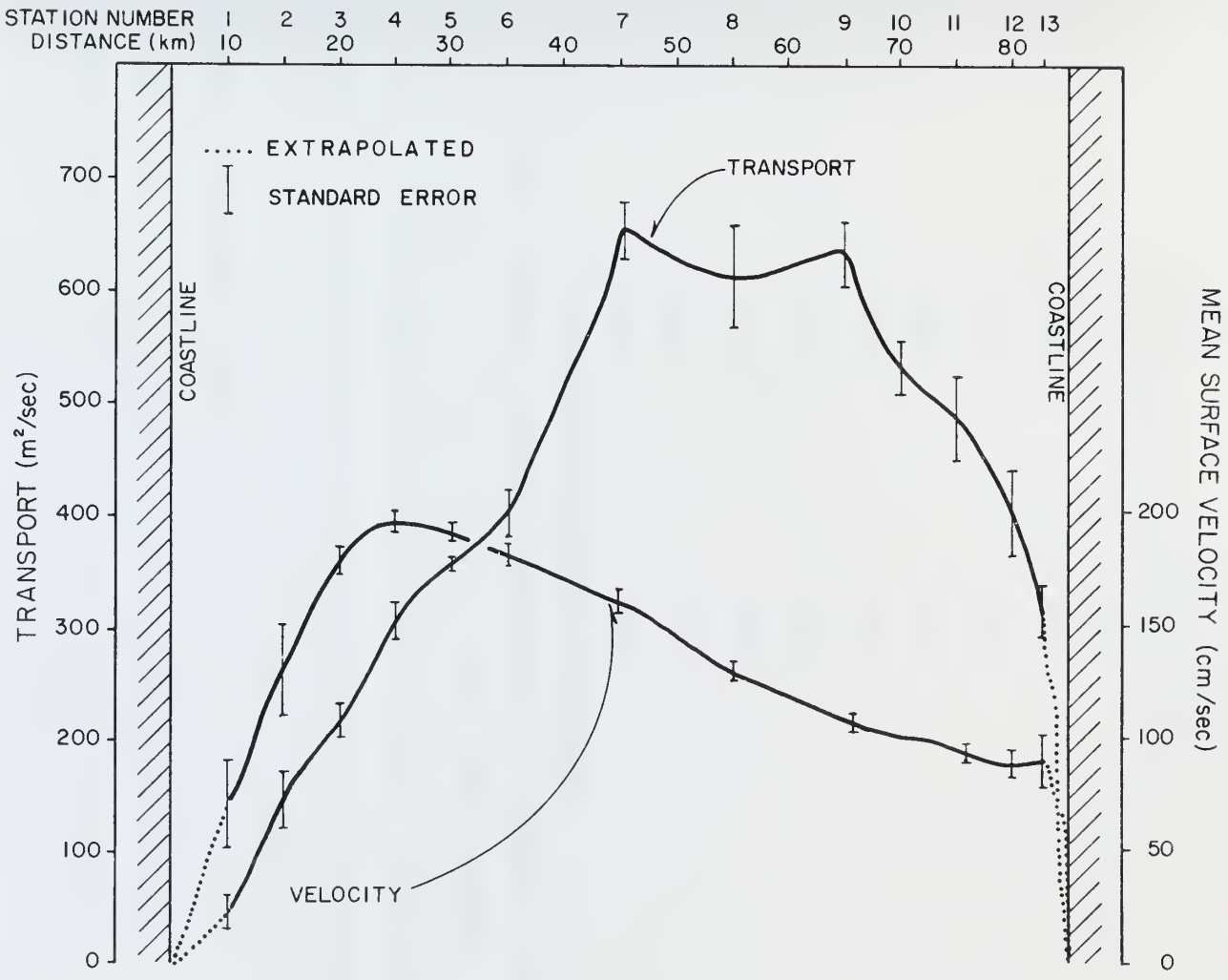

Figure 22. Mean observed downstream transport (m^3/sec) and surface velocity (cm/sec) with standard errors.

The volume transport for each of the nine days was computed separately and is shown in the table below. The average of these nine values is 33.4 x 10^6 m^3/sec.

Date	Volume transport (x 10^6 m^3/sec)
27 May	30.3
28 May	33.3
29 May	34.7
30 May	33.2
31 May	36.8
1 June	31.2
2 June	36.5
3 June	31.3
4 June	32.9

Continuous electrode potential measurements of transport based on two electrodes located at stations 2 and 3 showed good agreement with the free-fall measurements during the nine day period. The directly measured and electrode measured transport differed by less than 10%, but tidal aliasing of the free-fall measurements precludes any firm conclusion (DeFerrari, 1970).

(6) The cross-stream data is not of sufficient quality for a detailed analysis of the mean cross-stream velocity structure. A general pattern can be ascertained by the differentiation of the mean transport curves. On the cyclonic side, the velocity is westward except for a mid-depth layer (50-70 meters thick) of eastward flow. On the anticyclonic side, the velocity is eastward in the upper 400-500 meters and westward below this depth.

The mean cross-stream transport is shown in Figure 23, where positive values indicate eastward transport and negative values, westward transport. There is westward transport in the westward side of the Straits, eastward flow in the eastern side of the Straits, and, hence, an area of divergence near the center. The mean patterns are statistically significant at the 95% level.

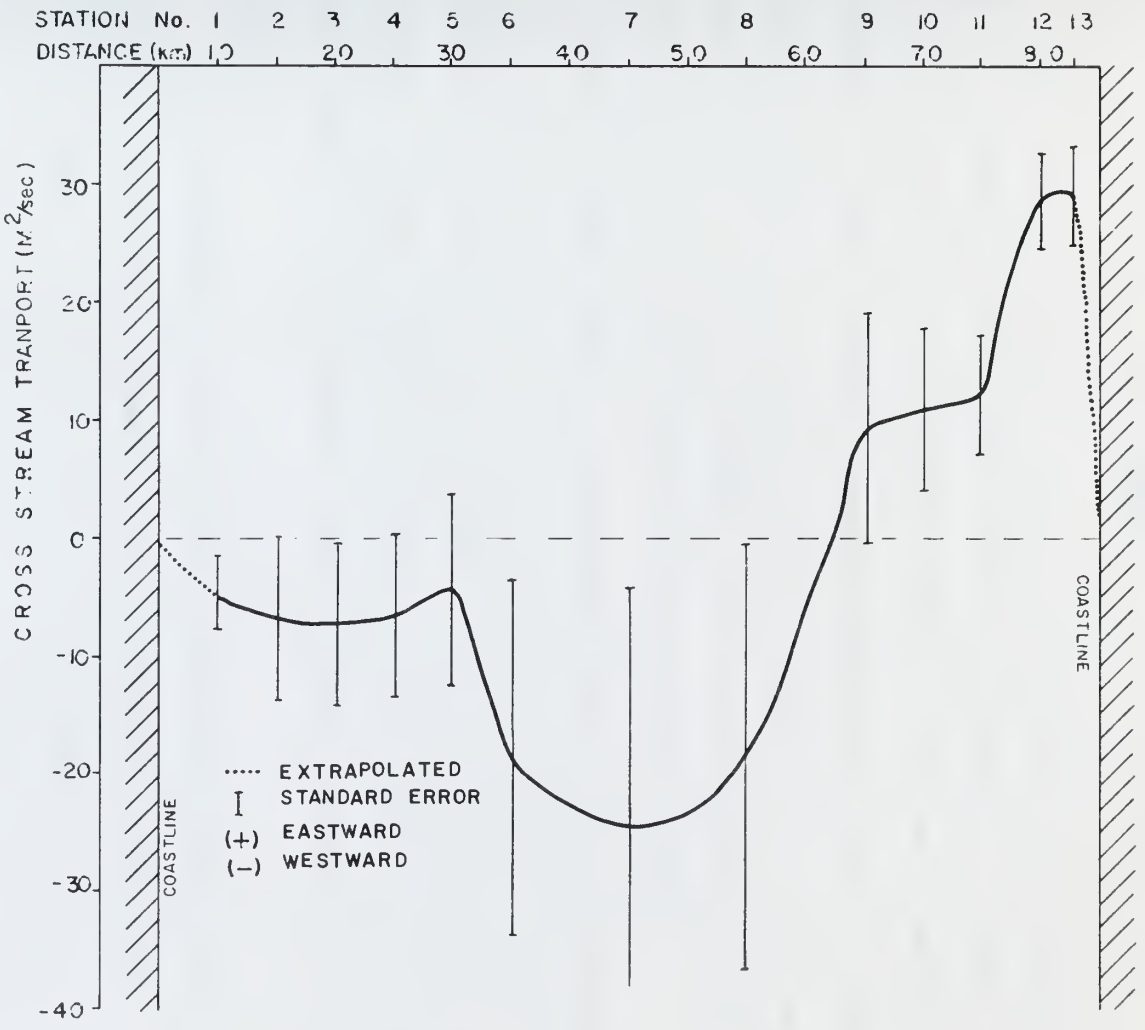

Figure 23. Mean observed cross-stream transport (m^3/sec) with standard errors.

IV. SUMMARY AND CONCLUSIONS

A. SUMMARY

Nine consecutive days of free-fall, STD data, taken by Richardson during late May and early June of 1969, were analyzed in a study of the baroclinic structure of the Florida Current. The directly measured transport was used to obtain the mean velocity field, and the directly measured temperature and salinity profiles were used to obtain the mean density field. Mean (i.e. averaged over the nine day period) vice daily values were used to reduce the tidal aliasing problem.

The mean axial velocity was southward beneath the Florida Current during the nine day period. This indication of southward flow was consistent with Hurley (1963), Neumann (1970), Düing and Johnson (1971), and Düing (1971). Richardson, Schmitz and Niiler (1969) did not find this southward flow as permanent feature when more extensive data were analyzed.

For the geostrophic calculations, three methods were used to determine the depth of no motion: the depth where the observed velocity equals zero, equating the geostrophic and observed velocities at the surface, and Defant's method. On the cyclonic side, there was good agreement between the depths of no motion determined by the three methods, and on the anticyclonic side the agreement was not so good. Likewise, on the cyclonic side Defant's method showed a definite depth of no motion, but on the anticyclonic side the results were less

conclusive.

Using the hybrid depth of no motion, the geostrophic velocity field was computed. The comparison of the observed and computed velocity fields showed good agreement on the cyclonic side and much less agreement on the anticyclonic side. The same pattern of agreement between absolute values existed in the comparison of surface velocities and of velocity and transport profiles at several stations. The thermal wind equation was shown to be a good approximation, i.e. the flow was essentially geostrophic throughout the Straits. The greatest discrepancies occurred in the area of the southward flow and in the easternmost part of the anticyclonic zone of the Straits. The discrepancy may be related to the limitations of the observational and data analysis techniques.

Also, the study of the standard deviation of temperature, salinity and σ_t showed a zone of high variability on the cyclonic side.

The study of stability parameters showed an area of low dynamic and baroclinic stability on the cyclonic side.

B. CONCLUSIONS

(1) The validity of the free-fall, STD measurements was established by comparison with previous total transport values.

(2) The Defant method was a valid method for determination of a depth of no motion on the cyclonic side. The bottom was a reasonable depth of no motion on the anticyclonic side. Thus, absolute geostrophic velocities can be computed independent of a direct method for depth of no motion determination.

(3) The Florida Current was essentially in geostrophic balance.

(4) A southerly flow beneath the Florida Current was confirmed during the nine day period. The T-S curve of the mid-channel southward flow has shown the salinity minimum that is characteristic of the Antarctic Intermediate Water. If a steady countercurrent existed, different T-S curves would be likely. In the vicinity of this countercurrent, the net transport between isopycnals was substantially to the north. The lack of net southward transport, and of a distinction in the T-S correlations, precluded resolving whether a large eddy or a steady countercurrent exists on the basis of the present data. Richardson, Schmitz and Niiler (1968) showed that, over a longer time span, the north component of velocity fills the whole channel, which implies a transient nature for the southerly flow. The velocity profile analysis by Düing and Johnson (1971) and Düing (1971) gave definite indications of a transient southerly flow with reversals on a time scale as short as a day.

Based on the present data and the previous works cited, the southward flow appeared to be of a transient nature and southerly origin.

(5) The free-fall, STD method provided the synoptic measurement of the velocity and density fields necessary for a study of the baroclinic structure of the Florida Current. Due to the tidal aliasing problem, time averaged mean values must be used.

There are numerous other techniques that could have been used to process and analyze the free-fall, STD data. Some examples are: use of some other order of polynomial besides cubic; use of the spline technique for curve fitting rather than least squares technique;

fitting a polynomial to the raw (i.e. the actual values of transport measured) data to obtain a mean transport curve; and direct differentiation of the mean, or individual, transport curves rather than of the polynomial representative of the curves. Additionally, the same curve fitting technique used with the observed transport curve could be applied to the geostrophic transport curve. This would make the comparisons between the computed and observed quantities more uniform.

Because of the uncertainties in determining the "best" technique, more emphasis in the future should be given to statistical and error analyses. Despite the lack of these analyses, the results of this thesis gave a realistic nine day mean description of the baroclinic structure of the Florida Current.

LITERATURE CITED

BROIDA, S., 1969. Geostrophy and direct measurements in the Straits of Florida. J. Mar. Res., 27 (3) : 278-292.

DEFANT, A., 1941. Die absolute Topographie des physikalischen Meeresniveaus und der Druck flächen, sowie die Wasserbewegungen im Atlantischen Ozean. Meteor-Werk, 6 (2) : 191-260.

DEFERRARI, H.A., 1970. Dynamically induced fluctuations in acoustic transmissions. Rosenstiel School of Marine and Atmospheric Science, University of Miami, Technical Report No. ML 70116, 88 pp.

DÜING, W., 1971. Unpublished data from Project SYNOPS (synoptic observation of current profiles in the Straits). June 1971. (personal communication).

DÜING, W., AND D. JOHNSON, 1971. Southward flow under the Florida Current. Science (in press).

FORMIN, L.M., 1964. The Dynamic Method in Oceanography. Elsevier Pub. Co., New York., 212 pp.

HURLEY, R.J., AND L.K. FINK, 1963. Ripple marks show that counter-current exist in Florida Straits. Science, 139 (3555) : 603-605.

MOOERS, C.N.K., 1970. CHARSECT computer program. (personal communication).

1971. Several effects of baroclinic currents on the cross-stream propagation of inertial-internal waves. Submitted to Geophys. Fluid Dynamics.

NEUMANN, A.C., AND M.M. BALL, 1970. Submersible observations in the Straits of Florida: geology and bottom currents. Geol. Soc. Amer., 81 : 2861-2874.

NEUMANN, G., AND W.J. PIERSON, JR., 1966. Principles of Physical Oceanography. Prentice-Hall, Inc., London, 545 pp.

O'BRIEN, F.J., III, 1967. On the validity of the geostrophic approximation for the Florida Current. Masters Thesis, University of Miami, 46 pp.

PILLSBURY, J.E., 1890. The Gulfstream - A description of the methods employed in the investigation and the results of the research. U.S. Coast and Geodetic Survey Publ. Report 1890, Appendix No. 10, pp. 44-620.

RICHARDSON, W.S., AND W.J. SCHMITZ, JR., 1965. A technique for the direct measurement of transport with application to the Straits of Florida. J. Mar. Res., 23 : 172-185.

RICHARDSON, W.S., AND W.J. SCHMITZ, JR., 1968. On the transport of the Florida Current. Deep-Sea Res., 15 (6) : 679-693.

RICHARDSON, W.S., W.J. SCHMITZ, JR., AND P.P. NIILER, 1969. The velocity structure of the Florida Current from the Straits of Florida to Cape Fear. Deep-Sea Res., Suppl. 16 : 225-231.

SANDSTRÖM, J.W., AND B. HELLAND-HANSEN, 1903. Über die Berechnung von Meerestromungen. Rept. on Norwegian Fishery and Marine Investigations, 2 (4) : 1-43.

SCHUREMAN, P., 1958. Manual of Harmonic Analysis and Prediction of Tides. U.S. Government Printing Office, Washington, D.C., 317 pp.

SMITH, J.A., B.D. ZETLER AND S. BROIDA, 1969. Tidal modulation of the Florida Current surface flow. Mar. Tech. Soc. J., 3 (3) : 41-46.

STOMMEL, H., 1958. The Gulf Stream, a physical and dynamical description. University of California Press, Berkeley, 202 pp.

WENNEKENS, M.P., 1969. Water mass properties of the Straits of Florida and related waters. Bull. Mar. Sci. Gulf Caribbean, 9 (1) : 1-52.

WUST, G., 1924. Florida - und Antillenstrom. Veröff. Inst. f. Meereskunde. Univ. Berlin Reihe A, 12 : 1-70.

APPENDIX A

Tidal Aliasing Computations

The average crossing time for a transect was about 8 hours. Because of the distorting influence of the periodic tidal forces, it was necessary to work with mean values averaged over the nine days rather than daily values. As shown in Table II, the station times were varied as practicable by starting a transect at Miami and Bimini on alternate days in an effort to reduce the tidal aliasing.

Because of the short record length, a tidal analysis was not possible. The following method was used to determine the tidal aliasing effect.

For the diurnal tide, consider

$$\alpha = \frac{1}{N} \sum_{j=1}^{N} [\sin(2\delta tj)] \sin(\sigma tj + \theta) ,$$

and for the semidiurnal tide

$$\beta = \frac{1}{N} \sum_{j=1}^{N} [\cos^2(\delta t)] \sin 2(\sigma tj + \theta),$$

where

$\alpha(\beta)$ is the normalized error in the mean, computed over N samples due to a diurnal (semidiurnal) constituent;

$\delta = \frac{2\pi}{27.3(24)}$: lunar declination frequency (radians/hour);

$\delta = \frac{2\pi}{365(24)}$: solar declination frequency (radians/hour);

$\sigma = \frac{2\pi}{25}$: lunar tidal frequency (radians/hour);

$\sigma = \frac{2\pi}{24}$: solar tidal frequency (radians/hour);

N is the number of observations for a particular station;

tj is the time of each observation for a particular station;

and, θ is the phase angle.

The phase angle θ was determined from the difference between the value of equilibrium argument $(V_0 + u)$ of a constituent when $t = 0$ and the epoch of a constituent (κ). The values of $(V_0 + u)$ were determined from Schureman (1958) and values of κ from Smith, Zetler and Broida (1969).

Using the four constituents K_1, O_1, M_2 and S_2, the velocity error, ΔV, of the mean observed velocity due to the diurnal (lunar, solar) and semidiurnal (lunar, solar) tides was computed:

$$\Delta V_{\text{Diurnal(lunar,solar)}} = \alpha \frac{V_T}{V_0} ,$$

and

$$\Delta V_{\text{Semidiurnal(lunar,solar)}} = \beta \frac{V_T}{V_0} ,$$

where

α, β are the factors described previously,

V_T is the current speed of a tidal constituent determined from Smith, Zetler and Broida (1969),

and, V_0 is the "average" current speed of the water column estimated by taking ½ of the mean observed surface velocity.

The values of the parameters used in the calculations and the resultant values of % velocity error (ΔV) are shown in the tables below:

Tidal constituent	K_1	O_1	M_2	S_2
Epoch of constituent (κ)	24^o	12^o	115^o	309^o
Velocity of constituent (V_T) cm/sec	5.7	5.6	3.4	2.5

Station Number	1	2	3	4	5	6	7
Velocity of water column (V_T) cm/sec	33	68	92	98	96	89	80
Normalized error (α), diurnal, lunar	-.15	-.27	-.30	-.27	-.37	-.41	-.40
Normalized error (α), diurnal, solar	.51	.59	.67	.72	.80	.84	.84
Normalized error (β), semidiurnal, lunar	.03	.03	.07	.06	.08	.06	.12
Normalized error (β), semidiurnal, solar	-.31	-.17	-.08	-.06	.17	.32	.40
% Velocity error (ΔV)	4.3	2.3	2.4	2.7	3.3	3.9	4.9

Station Number	8	9	10	11	12	13
Velocity of water column (V_T) cm/sec	63	54	51	45	42	41
Normalized error (α), diurnal, lunar	-.36	-.21	-.22	-.17	-.17	-.04
Normalized error (α), diurnal, solar	.68	.70	.49	.35	.33	.26
Normalized error (β), semidiurnal, lunar	.24	.02	.00	.00	-.01	-.03
Normalized error (β), semidiurnal, solar	.24	.21	-.18	-.27	-.32	-.23
% Velocity error (ΔV)	5.2	6.6	2.1	0.9	0.1	1.9

Hence, the error in mean observed velocity values due to tidal biasing is about 3%. Also, as anticipated, errors due to diurnal tides predominate those due to semidiurnal tides and the error is greatest in mid-channel.

VITA

LCDR William O. Stubbs, Jr., USN, was born in Statesboro, Georgia, on 2 November 1939. His parents are the late William O. Stubbs, Sr., and Penny Anne Stubbs. He received his elementary education in Statesboro Grammar School, Statesboro, Georgia, and his secondary education in Statesboro High School.

In July 1958, he entered the U.S. Naval Academy, Annapolis, Maryland. Upon graduation in June 1962, with a B.S., he was commissioned an Ensign in the U.S. Navy. Subsequent naval service included two years in the Mine Force of the Atlantic Fleet, three years in the Destroyer Force of the Atlantic Fleet, and one year in the River Patrol Force in South Vietnam.

He was admitted to the Graduate School of the University of Miami in January 1969. He was granted the degree of Master of Science in July 1971.

He is married and has three children.

Permanent address: College Boulevard
Statesboro, Georgia 30458

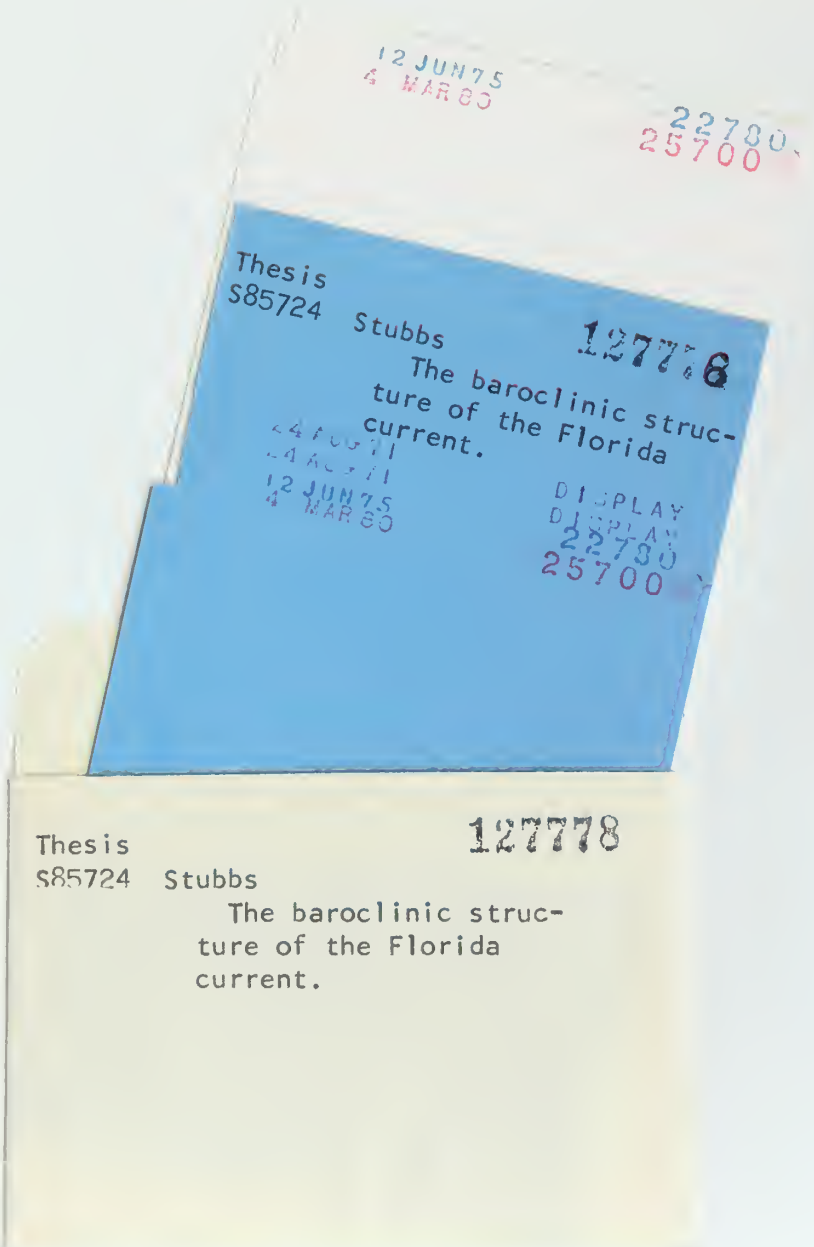

Thesis
S85724 Stubbs
127778
The baroclinic structure of the Florida current.